

**Accumulation of Low Density Lipoprotein (LDL) in Diseased Artery**

by

Nurulain Amelia binti Mohd Razmi

Dissertation submitted in partial fulfillment of  
the requirements for the  
Bachelor of Engineering (Hons)  
(Chemical Engineering)

MAY 2012

University Teknologi PETRONAS  
Bandar Seri Iskandar  
31750 Tronoh  
Perak Darul Ridzuan

CERTIFICATION OF APPROVAL

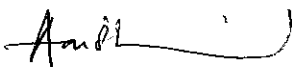
**Accumulation of Low Density Lipoprotein (LDL) in Diseased Artery**

by

Nurulain Amelia binti Mohd Razmi

A project dissertation submitted to the  
Chemical Engineering Programme  
Universiti Teknologi PETRONAS  
in partial fulfilment of the requirement for the  
BACHELOR OF ENGINEERING (Hons)  
(CHEMICAL ENGINEERING)

Approved by,



(Dr Anis Suhaila bt Shuib)

UNIVERSITI TEKNOLOGI PETRONAS

TRONOH, PERAK

May 2012

## CERTIFICATION OF ORIGINALITY

This is to certify that I am responsible for the work submitted in this project, that the original work is my own except as specified in the references and acknowledgements, and that the original work contained herein have not been undertaken or done by unspecified sources or persons.



---

NURULAIN AMELIA BINTI MOHD RAZMI

## **ACKNOWLEDGEMENT**

My utmost gratitude goes to the Almighty God whom without His help by giving good health and time, I am unable to finish my project successfully.

This project would not be completed successfully without the assistance and guidance from individuals. Therefore, I owe my deepest gratitude to my supervisors, Dr Anis Suhaila bt Shuib for her guidance, patience, support and encouragement.

Sincerest gratitude goes to Mr Abdul Rashid bin Haji Serakawi for his patience, invaluable input and guidance in ANSYS FLUENT 14.0 training. Not only that, many thanks to laboratory technical support for dealing with and solving the computing problems.

To the Final Year Research Paper and Project Coordinators, Dr Anis Suhaila bt Shuib (FYP I) and Dr Norhayati Mellon (FYP II), thank you for coordinating the series of training and talks and quick announcements, information and respond toward the project completion.

I thank all staffs of Chemical Engineering Department intentionally and unintentionally for any guidance and information regarding this course.

Lastly, for their everlasting love and warm hearted support, I thank my grateful family and my friend who is willing to lend their ears to hear my problem and giving continuous support in completing this project.

## ABSTRACT

A cardiovascular disease such as heart attacks, strokes and hypertension is the primary cause of deaths around the world. The atherosclerosis progression is where the artery becomes hardening due to accumulation of bad cholesterol also known as low density lipoprotein (LDL).

This project is modeled and simulated by using the ANSYS 14.0 software package. The stenosis artery with 30% reduction with total length is 22 mm and 2 mm of diameter aligned in position x-axis. Then, stenosis tube is modeled and being put in meshing before setting up the solver.

The solver is setting up with Spalart Allmaras model in order to study the blood flow behavior. The study were involved the characterization of blood flow under steady state mode and the inlet velocities were 0.18 m/s, 0.2 m/s, 0.3 m/s, 0.4 m/s and 0.5 m/s. The Discrete Phase Model is used to consider the LDL particle motion in blood flow and the LDL size that put into consideration during the study was 1  $\mu\text{m}$ , 3  $\mu\text{m}$  and 5  $\mu\text{m}$ .

The finite volume method is used to solve Navier stoke (NS) equation as governing equation as well as the particle motion equation which it is demonstrated the LDL particle movement in the stenosis artery.

From the studies, it has been found that high velocity will create the recirculation region. Thus, LDL particle will travel longer than low velocity, which means it long residence time of LDL particle. Thus, the chance of LDL accumulation near the artery wall is high. The study also shows that the size of lipid particle effect the atherosclerosis progression significantly. It can be said that, big size of LDL give a great impact to the atherosclerosis progression.

The finding of this project has proved that parameters, LDL residence time and LDL size have a great contribution toward the atherosclerosis progression. But, mass transfer of LDL did not take into account and the study of it is considerable to be employed in a future.

## **Table of Contents**

CERTIFICATION OF APPROVAL	II
CERTIFICATION OF ORIGINALITY	III
ACKNOWLEDGMENT	IV
ABSTRACT	V
LIST OF TABLE	VIII
LIST OF FIGURES	VIII
LIST OF ABBREVIATIONS	X
CHAPTER 1: INTRODUCTION	1
1.1 Background of Study	1
1.1.1 Cardiovascular Diseases	1
1.1.2 Worldwide Statistic	1
1.1.1.2 WHO Statistic	1
1.1.1.3 Malaysia Statistic	2
1.1.3 Atherosclerosis	3
1.1.4 Definition of LDL	5
1.2 Problem Statement	6
1.3 Objectives	6
1.4 Scopes of Study	6
CHAPTER 2: LITERATURE REVIEW & THEORY	7
2.1 Literature Review	7
2.1.1 Blood Flow Behavior	7
2.1.2 Mechanism of LDL	7

2.2	Theory	8
2.2.1	Hagen Poiseuille Flow	10
2.2.2	Navier stokes Equation	10
2.2.2.1	Conservation of mass	10
2.2.2.2	Conservation of momentum	11
2.2.2	The Equation of Continuity	11
2.2.3	Particle Motion Equation	12
2.2.4	Characteristic of Flow	13
2.3	Summary	14
	CHAPTER 3: RESEARCH METHODOLOGY	15
3.1	Computational Fluid Dynamic (CFD)	15
3.2	Research Methodology	16
3.2.1	Define the modeling objectives	16
3.2.2	Create model geometry	16
3.2.3	Meshing	18
3.2.4	Setup the solver and physical models	18
3.3	Project Milestone	21
	CHAPTER 4: RESULT AND DISCUSSION	23
4.1	Flow Movement at Inlet Velocity 0.18 m/s	23
4.2	Flow Movement at Inlet Velocity 0.20 m/s	25
4.3	Flow Movement at Inlet Velocity 0.30 m/s	27
4.4	Flow Movement at Mean Velocity 0.40 m/s	29
4.5	Flow Movement at Mean Velocity 0.50 m/s	31
4.6	The study of LDL size variation in corresponding to LDL accumulation.	34

CHAPTER 5: CONCLUSION AND RECOMMENDATIONS	36
5.1 Conclusion	36
5.2 Recommendation	37
REFERENCES	38
APPENDICES	41
Appendix A1 Glossary	41
Appendix B1 Derivation of Navier Stokes Equation	42

### **List of Tables**

Table 1: Reynold's Number by Literature	13
---	----

### **List of Figures**

Figure 1: Distribution of death by leading cause group, male and female. Source: The Global Burden of Disease, WHO.	2
Figure 2: 10 Principles causes of Death in Malaysia	3
Figure 3: The Artery Condition	4
Figure 4: Flowchart of Plaque Formation	5
Figure 5: The schematic drawing of formation of concentration polarization.	8
Figure 6: Hagen Poiseuille Flow Concept	8
Figure 7: Mass flux balance	10
Figure 8: FLUENT operation system	15
Figure 9: Research Methodology	16
Figure 10: Diseased Artery Geometry	17
Figure 11: Normalized Scale	17



Figure 12:	Quadrilateral grid mesh	18
Figure 13:	Normal Cardiac Cycle	19
Figure 14:	Scaled Residual	20
Figure 15:	Project Milestone	22
Figure 16:	Velocity (a) contour (b) vector (c) LDL residence time at inlet velocity 0.18 m/s	23
Figure 17:	Velocity (a) contour (b) vector (c) LDL residence time at inlet velocity 0.2 m/s	25
Figure 18:	Velocity (a) contour (b) vector (c) LDL residence time at inlet velocity 0.3 m/s	27
Figure 19:	Velocity (a) contour (b) vector (c) LDL residence time at inlet velocity 0.4 m/s	29
Figure 20:	Velocity (a) contour (b) vector (c) LDL residence time at inlet velocity 0.5 m/s	31
Figure 21:	Graph of velocity versus residence time at recirculation region.	33
Figure 22:	Graph of LDL size versus LDL residence time at inlet velocity 0.4 m/s	34
Figure 23:	Graph of LDL size versus LDL residence time at inlet velocity at 0.5 m/s	34
Figure 24:	LDL size versus LDL residence time at two velocities	35
Figure 25:	Types of Computational Modelling of Porous Media	37

## **List of Abbreviations**

CVD	Cardiovascular diseases
CFD	Computational Fluid Dynamics
LDL	Low density lipoprotein
NS	Navier Stoke
WHO	World Health Organization

# CHAPTER 1

## INTRODUCTION

### 1.1 Background of Study

#### 1.1.1 Cardiovascular Diseases

Unhealthy standards of living such as tobacco use, physical inactivity and as unhealthy diet are main contribution to the risk of having cardiovascular diseases (CVD). Cardiovascular disease (CVD) is group of disorder of heart and blood vessel and become the number one cause of death globally.

The condition when the blood circulation in vital organs (heart and brain) is blocked has lead to the heart attack or stroke. Once the blockage occurs the heart muscle and brain cells become damage due to lack of blood supply.

#### 1.1.2 Worldwide Statistic

##### *1.1.1.2 WHO Statistic*

WHO statistic had shown that approximately 17.3 million people died from CVDs in 2008, representing 30% of all global deaths and from these numbers, 7.3 million deaths due to coronary disease and stroke cause approximately 6.2 million of deaths. By projection, almost 23.6 million people around the world will die from CVDs, mainly from heart disease and stroke in 2030 (*Cardiovascular diseases (CVDs)*, 2011).

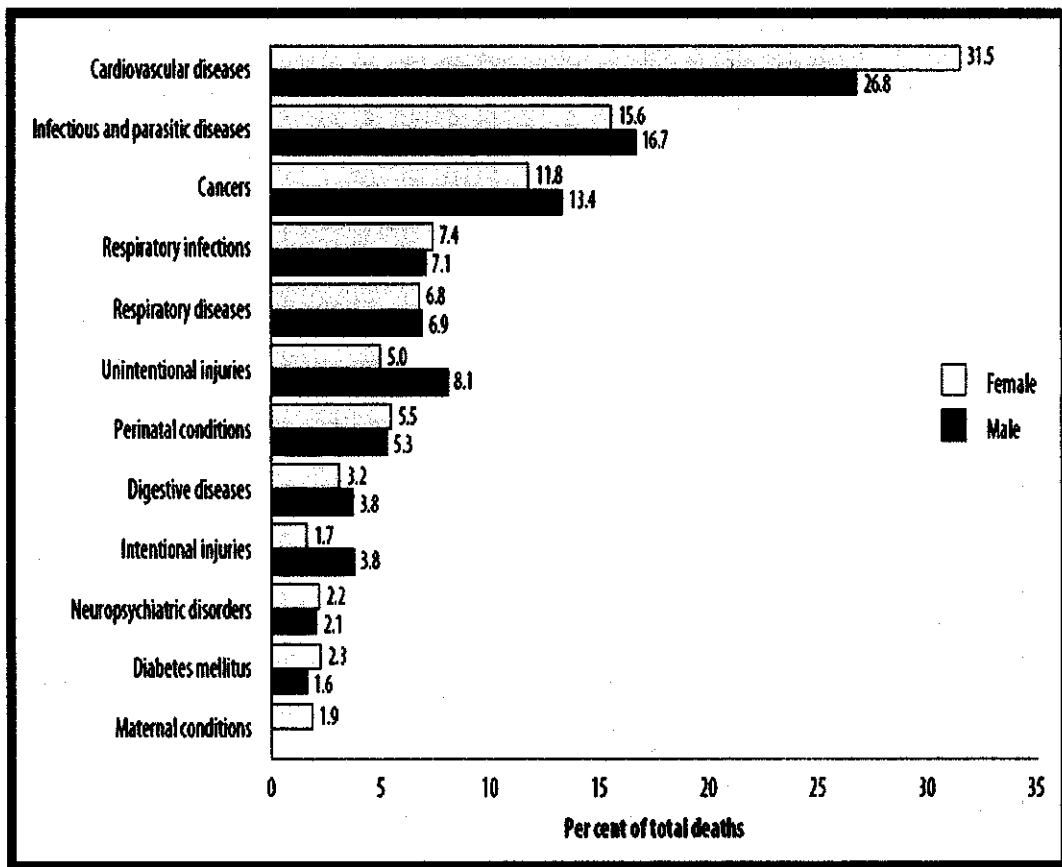


Figure 1: Distribution of death by leading cause group, male and female. Source: The Global Burden of Disease, WHO

From figure 1 above, cardiovascular diseases contribute more than half, about 58.3% of total deaths and from the percentage of total deaths, women contribute 31.5% of it. Apparently, the insufficient physical activity and unhealthy diet may lead to this disease.

### 1.1.1.3 Malaysia Statistic

In Malaysia, statistic in 2009 from the Health Ministry reported that about one in four deaths in government hospitals are suffered from heart or strokes. From both statistics, the number of death causing by the cardiovascular disease are not likely improve in the coming year. In addition, the poor lifestyle habit of the societies such as smoking, regular alcohol intake, imbalance food consumption as well as inadequate exercise contributes to the current problem (Hooi, 2012).

10 Sebab Kematian utama . Malaysia, 2006 10 Principal Causes of Death, Malaysia, 2006			
Disahkan <i>Medically certified</i>	%	Tidak disahkan <i>Not medically certified</i>	%
1. <i>Ischaemic heart disease</i>	12.0	1. Sakit tua 65+ <i>Old age 65+</i>	57.9
2. <i>Septicaemia</i>	7.1	2. Lelah <i>Asthma</i>	7.3
3. <i>Cerebrovascular disease</i>	7.0	3. Barah <i>Cancer</i>	7.1
4. <i>Transport accident</i>	5.7	4. Sakit jantung <i>Heart disease</i>	5.8
5. <i>Pneumonia</i>	5.4	5. Kencing manis <i>Diabetes</i>	3.5
6. <i>Chronic lower respiratory disease</i>	2.4	6. Jangkitan kuman <i>Viral infection</i>	2.4
7. <i>Malignant neoplasm of trachea, bronchus and lung</i>	2.2	7. Darah tinggi <i>Hypertension</i>	1.7
8. <i>Diabetes mellitus</i>	2.1	8. Angin ahmar <i>Stroke</i>	1.2
9. <i>Certain conditions originating in the perinatal period</i>	1.6	9. Penyakit berjangkit <i>Infectious disease</i>	1.0
10. <i>Congenital malformations, deformations and chromosomal abnormalities</i>	1.4	10. Sakit buah pinggang <i>Kidney disease</i>	1.0
Keseluruhan sebab <i>All causes</i> (68,124)		Keseluruhan sebab <i>All causes</i> (46,960)	

Figure 2: 10 Principles causes of Death in Malaysia

Figure 2 above shows causes of death in Malaysia and types of CVD which are isohaemic heart disease and cerebrovascular disease under top five of cause of death in Malaysia.

### 1.1.3 Atherosclerosis

In a scientific term, CVD is occurring due to atherosclerosis, hardening of arteries due to abnormal accumulation of low density lipoprotein (LDL) in the artery wall.

It occurs due to deposition of fatty substances; cholesterol, cellular waste products, calcium and other substances build up in the inner of artery. The figure below shows the artery condition of mild and severe atherosclerosis compare to normal artery.

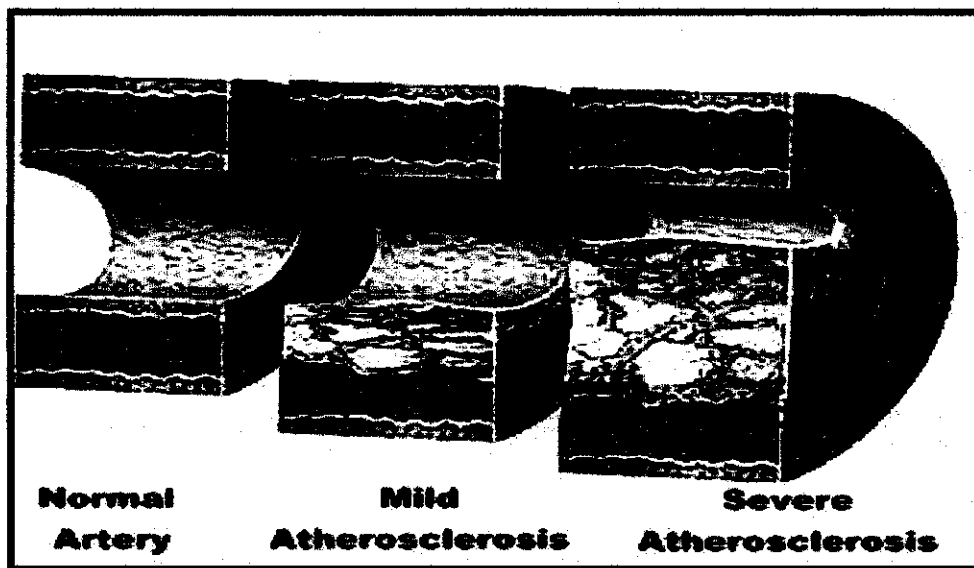


Figure 3: The Artery Condition

The cholesterol particles infiltrate into damaged artery wall which it has three layers. The abnormal accumulation of LDL will lead to the formation of plaque and it narrows the artery and make harder for blood to flow.

The plaque deposit in the artery will cause the atherosclerosis lesion. Atherosclerosis lesion can be found preferentially at specific sites in the arterial system, particularly near the bend, bifurcations and some other region which is identified by complicated blood flow pattern (Ethier, 2002). The figure below shows the plaque formation in the artery as been discussed above.

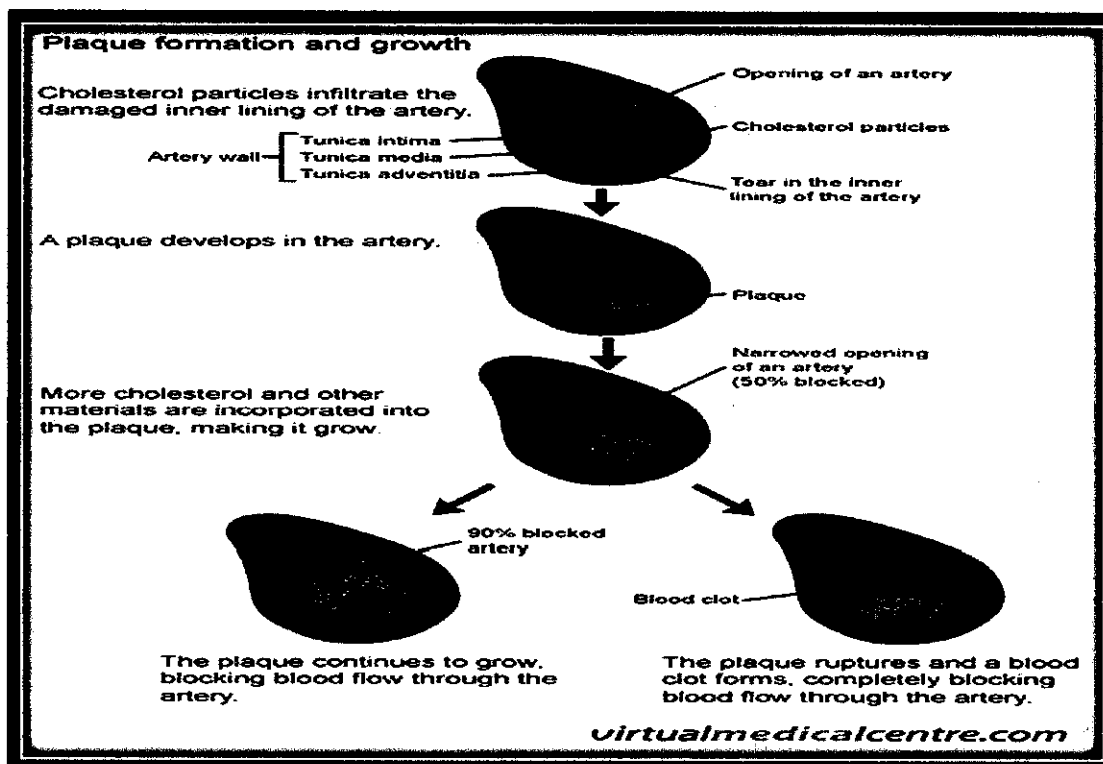


Figure 4: Flowchart of Plaque Formation

#### 1.1.4 Definition of LDL

Low Density Lipoprotein (LDL) and High Density Lipoprotein (HDL) are two types of cholesterol. But LDL particles are frequently referred to as bad cholesterol. Studies have shown that higher levels of LDL in blood promote health problems.

It has the shape of spherical and has variation in size and density. According to Sacks (2003), the size and density of LDL particles depend on how much is the core and the natural content of LDL, respectively. The size of LDL particles has the link to atherosclerosis progression (Varady et al., 2011) (Sacks & Campos, 2003). The mechanism that link LDL particles to atherosclerosis progression are that they have long residence time in plasma, enhance oxidizability and increase the permeability through artery wall. (Superko et al., 2008) (Varady et al., 2011)

## **1.2 Problem Statement**

It is vital to understand blood behavior as it carries together the lipid throughout artery wall. The blood movement due to the plaque deposit become slower indicates the high risk of atherosclerosis. Therefore, the deposition of plaque into artery wall is also important to study.

There are few questions regarding what mechanism is exactly promote plaque deposition. The numbers of researcher papers are totally agreed about the correlation between wall shear stress and intimal thickening is not convincing enough to be put into consideration of this phenomenon (Kaazempur-Mofrad et.al, 2005). The blood flow in human body is a pulsatile flow where the velocity of blood is varying. The study need to be done in order to investigate the effect of LDL accumulation in each velocity. Also, the size of LDL particle that contribute to atherosclerosis remain debatable (Rizzo, 2006).

## **1.3 Objectives**

The objectives of the study are:

- To study the effect of velocity changes on LDL accumulation.
- To investigate the effect of LDL sizes that corresponding to LDL accumulation.

## **1.4 Scope of Study**

Finite volume method using ANSYS 14.0 will be employed to examine lipid accumulation. This study will involve the model of an artery with 30% reduction to represent a diseased artery. The study will be simulated under steady flow with four different inlet velocities which are 0.18 m/s, 0.2 m/s, 0.3 m/s, 0.4 m/s, 0.5 m/s. The observation of recirculation region on downstream of restriction area in each velocity will be analyzed with respect to the residence time. Secondly, the study of three sizes of LDL which are 1  $\mu\text{m}$ , 3  $\mu\text{m}$  and 5  $\mu\text{m}$  is simulated to examine the size of LDL particle that effect the atherosclerosis progression



## CHAPTER 2

### LITERATURE REVIEW & THEORY

#### 2.1 Literature Review

##### 2.1.1 Blood Flow Behavior

Consider a fluid is flowing inside a straight tube. The velocity of flow is not equal at all points as the highest velocity is at the center and drop at points toward the tube wall. The change of velocity is due to frictional force that occurs between adjacent layers of fluid and between the fluid and the tube wall. This frictional force arises from the viscous properties of the flowing fluid. Viscosity of fluid can be defined as the resistance to flow. Low viscosity occurs for small force on a fluid layer produces a high velocity of that layer relative to an adjacent layer. The theory of the viscosity can describe the rheology of blood.

According to Newton's law of viscosity, for laminar flow, *shear stress* ( $\tau$ ) is proportional to *shear rate* ( $\dot{\gamma}$ ).

$$\tau_w = \mu \cdot \dot{\gamma}_w \quad (1)$$

When shear rate is depended on dynamic viscosity,  $\mu$  it can be said as a non-Newtonian fluid. On the other hands, Newtonian fluid is defined as constant dynamic viscosity at all rates. Due to complexity of analyzing non-Newtonian fluid has forced many computational studies of flood flow to consider the whole blood as Newtonian fluid under specific condition (Katrtsis et al., 2007) even though the thought of blood as Newtonian fluid still under debate.

##### 2.1.2 Mechanism of LDL

The transportation of LDL to the artery wall involves mass transfer mechanism. It is fact that there is small amount of transmural flux of water from lumen to the adventitia of all arteries, caused by arterial pressure. Somehow, concentration polarization at apical surface of the endothelial cells might be occurred due to

diffusion of lipid to the endothelium cell. The concentration polarization can cause lipoprotein concentration to become higher in low shear region. So, it enhances the mass transfer of LDL into the artery wall. In Figure 4 below, it shows the LDL in blood flowing in artery with semipermeable wall. The formation of concentration polarization occurs due to transmemural fluid flux. (Ethier, 2002)

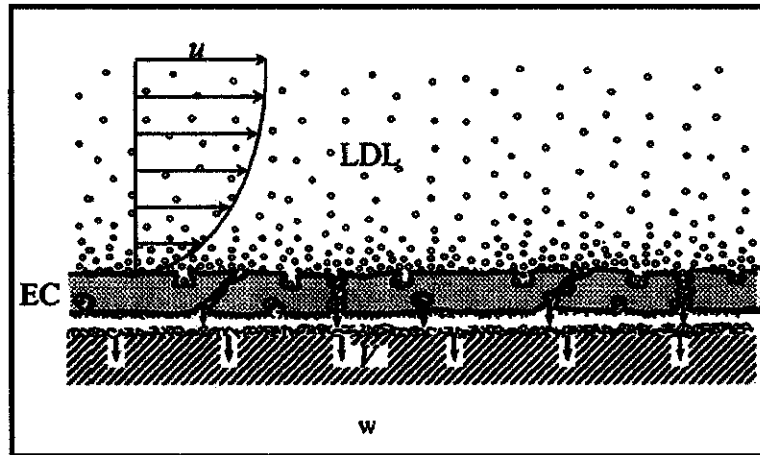


Figure 5: The schematic drawing of formation of concentration polarization.

## 2.2 Theory

### 2.2.1 Hagen Poiseuille Flow

The Hagen Poiseuille theory describes the characteristic in a straight and infinite cylindrical pipe. The principle is derived from the Navier Stoke equation. It relates pressure drop between the flow rates under the steady state flow.

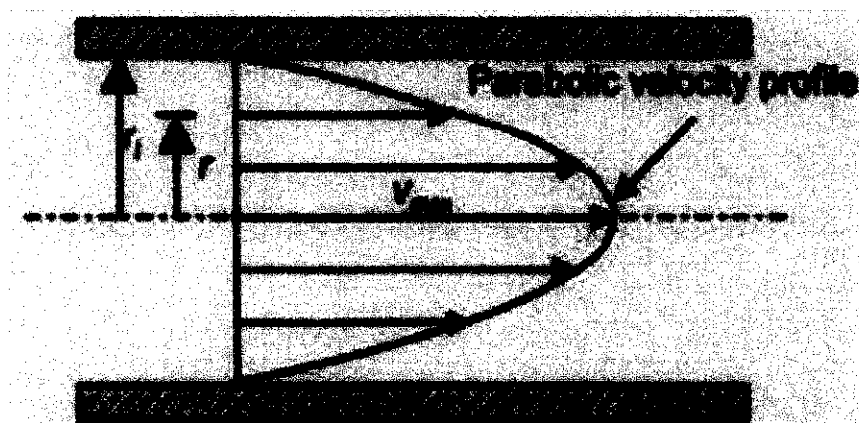


Figure 6: Hagen Poiseuille Flow Concept

The maximum point velocity,  $U_{\max}$  is at the center of the pipe,  $r = 0$ . The velocity profile as figure 7(a) can be expressed as

$$V = V_{\max} \left[ 1 - \left( \frac{r}{r_i} \right)^2 \right] \quad (1)$$

Where  $r_i$  is the pipe radius.

In a case of laminar and steady flow through a uniform tube of radius the velocity profile over the cross-section is a parabola. It also can be expressed as

$$v_r = \frac{\Delta P \cdot (r_i^2 - r^2)}{4 \cdot \eta \cdot l} \quad (2)$$

Where  $\Delta P$  is a pressure drop over the tube of length ( $l$ ), and  $\eta$  is blood viscosity.

$$Q = \frac{\Delta P \cdot \pi \cdot r_i^4}{8 \cdot \eta \cdot l} \quad (3)$$

Where  $Q$  is a flowrate.

There are the assumptions that need to be considered in this law, which are:

- The tube is stiff, straight, and uniform
- Blood is Newtonian, i.e., viscosity is constant
- The flow is laminar and steady, not pulsatile, and the velocity at the wall is zero (no slip at the wall).

The shear rate,  $\tau$  can be expressed as

$$\tau = \frac{dv}{dr} \quad (4)$$

In any related study of blood flow, the Hagen Poiseuille principle is used to explain the characteristic of blood flow in an artery. This relates to the drop of pressure because even small reduction in arterial diameter it will increase the amount of work the heart need to do, leading to a progressively stressed heart.

## 2.2.2 Navier Stokes Equation

Navier stokes equation is a set of nonlinear partial differential equations equation that describe the flow of fluid in whatever geometry either straight tube, cylindrical tube and et cetera.

This equation is a time dependent and derives from three conservation equations, conservation of mass, conservation of momentum and conservation of energy.

### 2.2.2.1 Conservation of mass

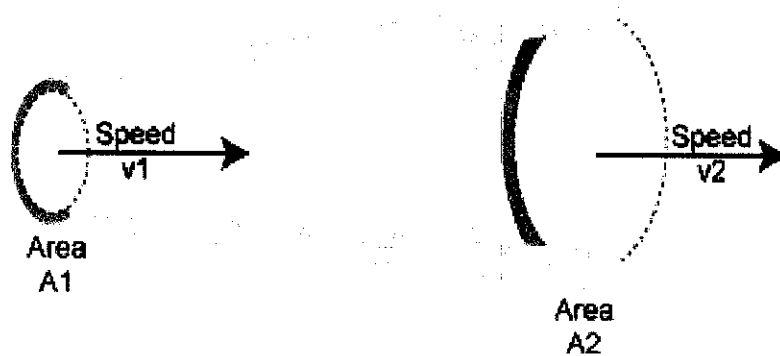


Figure 7: Mass flux balance

Consider an imaginary control volume and applying law of mass conservation is applied,

$$\text{Change of mass} = \text{Mass inlet} - \text{Mass outlet} \quad (1)$$

In above case,

$$\text{Mass inlet} = \int_{A1} \rho V1 \, dA \quad (2)$$

$$\text{Mass outlet} = \int_{A2} \rho V2 \, dA \quad (3)$$

By assumption that the fluid flow is incompressible indicates the constant density. Therefore, the rate of change in the control volume is zero. It can be described by the equation of continuity.

### 2.2.2.2 Conservation of momentum

Newton's 3<sup>rd</sup> law has stated that the forces are equal in magnitude and by applying Newton's 2<sup>nd</sup> law, the rate of change of momentum of a particle is proportional to the resultant force,  $F$  that acts on the particle. It gives the equation 2,

$$F = \frac{d(mv)}{dt} \quad (4)$$

Where the derivative is the time rate of change of momentum.

$$\begin{array}{ccccccc} \text{Rate of} & & \text{Rate of} & & \text{Rate of} & & \text{External} \\ \text{increase of} & = & \text{momentu} & - & \text{momentu} & + & \text{force on} \\ \text{momentu} & & \text{m in} & & \text{m out} & & \text{the fluid} \end{array} \quad (5)$$

The derivation of mass and momentum conservation will lead to the Navier Stokes equation.

$$\rho \frac{DV}{Dt} = -\nabla P + \mu \nabla^2 V + \rho g \quad (6)$$

The complete derivation is provided in Appendix B.

### 2.2.2 The Equation of Continuity

Blood is a viscous fluid mixture consisting plasma and cells. The component can be divided into three main cell types that each of it has its own function (Fournier, 2011). For this multi component mixture, continuity equation with constant density is applied.

$$\nabla \cdot \mathbf{v} = 0, \quad (\text{Incompressible flow}) \quad (7)$$

### 2.2.3 Particle Motion Equation

The particle motion equation is primarily derived from Newton's Second law where all forces,  $F$  act toward the particle is proportional to mass of a particle,  $m$  and acceleration,  $a$  of a particle.

$$F = ma \quad (8)$$

Lipid is a spherical particle and can be described in equation 9 below.

$$m_p \frac{dv_p}{dt} = m_p \left( 1 - \frac{\rho}{\rho_p} \right) g + F_{PG} + F_D + F_L + F_{VM} + F_{Bas} \quad (9)$$

Left hand side term indicates the particle inertia where  $M_p$  is the mass of particle,  $V_p$  is the velocity of the particle. Meanwhile, the right hand side term describes the forces caused by particle fluid interaction.

$F_D$  is the drag force can be described as equation 10 below. Drag force is needed to move the particle from constant fluid velocity

$$F_D = \frac{1}{2} \rho C_D \frac{\pi d^2}{4} V_s \quad (10)$$

Where  $C_D$  is a drag coefficient,  $d$  is the particle diameter and  $V$  is the relative velocity of particle and fluid.

$F_L$  is the lift force generated by rotation of particle and fluid shear. It can be occurred due to velocity gradient. To describe this phenomenon equation 11 is applied.

$$F_{LM} = \frac{\pi}{8} d_p^3 \rho \left[ \left( \frac{1}{2} \nabla \times V - \omega_p \right) \times V_s \right] \quad (11)$$

This equation is derived by Rubinow and Keller (1961).

$F_{PG}$  is the force that exists in the absence of the particle due to acceleration of the fluid and the hydrostatic pressure gradient,

$$F_{PG} = -V o_p \Delta p \quad (12)$$

where  $V_{op}$  is the particle volume and  $\nabla p$  is the pressure gradient produced by hydrostatic pressure.

$F_{vm}$  is defined as a virtual mass force accounts for the work required to change the momentum of the surrounding fluid as the particles accelerates and  $F_{Bas}$  is the unsteady drag force or Basset force which accounts for temporal development of the viscous region of the vicinity of the particles. These two terms do not have any significant effect in blood flow (Anis et.al, 2012).

### 2.2.4 Characteristic of Flow

The characteristic of blood flow can be indicated by the value of Reynold's number. Various studies related to diseased artery have been used different values of Reynold's number, depends on their problem of statement. Table 1 shows the value of Reynold's number by the previous research.

Table 1: Reynold's Number by Literature

Reynold's number	Condition
250 (Mofrad. K et al 2005)	<ul style="list-style-type: none"> <li>▪ Steady flow</li> <li>▪ 56% cross sectional area reduction</li> <li>▪ Rigid and stationary wall</li> <li>▪ <math>Sc = 3000</math></li> </ul>
250 (S. Fazli et al. 2011)	<ul style="list-style-type: none"> <li>▪ Pulsatile flow</li> <li>▪ 30% to 60% area of reduction</li> </ul>
10- 1000 (Ikbal et al, 2011)	<ul style="list-style-type: none"> <li>▪ 64% area reduction</li> <li>▪ Micropolar fluid</li> <li>▪ Different Re number shows different maximum shear rate and recirculation zone.</li> </ul>

### 2.3 Summary

The Hagen Poiseuille theory describes the characteristic in a straight and infinite cylindrical pipe. The principle is derived from the Navier Stoke equation. This equation will be used as a governing equation for solid liquid flows in which the forces involved in particle-fluid interaction that relevant to blood flow system have been discussed. The lift forces depend on the velocity gradient and vorticity of blood while the  $F_{vm}$  and  $F_{Bas}$  do not have significant effect in blood flow. The NS equation and particle motion equation will be solved simultaneously during simulation.



# CHAPTER 3

## RESEARCH METHODOLOGY

### 3.1 Computational Fluid Dynamic (CFD)

Computational fluid dynamic (CFD) is a general term used to describe the method that seeks the numerical solution of the governing equation, Navier Stokes for this case. The figure below shows the basic step while dealing with CFD.

FLUENT consists of mainly pre-processing step and solver. In a pre-processing, geometry is created. Software ANSYS 14.0 package come with creating geometry and meshing. Therefore, there is no need to use other type of software to create geometry and mesh.

Second phase is to select appropriate solver setting that subjected to the numerical model. From figure above, preprocessing output and solver setting is needed as input to the solver.

The solver will take into account the criteria such as material properties, boundary condition, and physical model in order to solve the governing equation. (*Chapter 3. basic steps for CFD analysis using FLUENT.2008*)

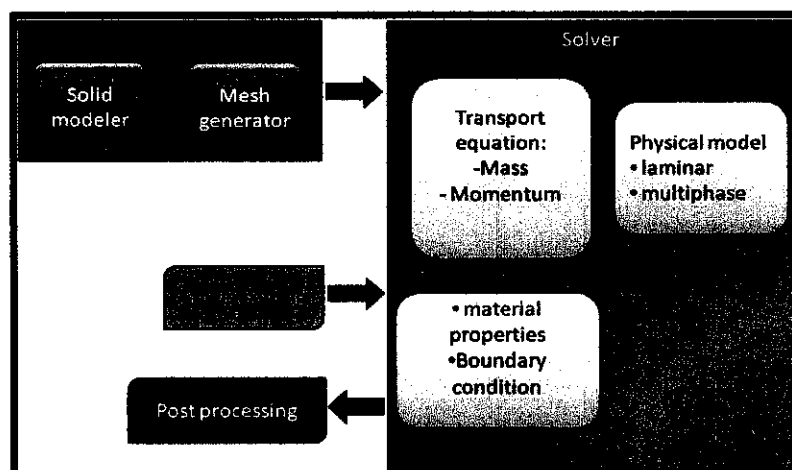


Figure 8: FLUENT operation system

## 3.2 Research Methodology

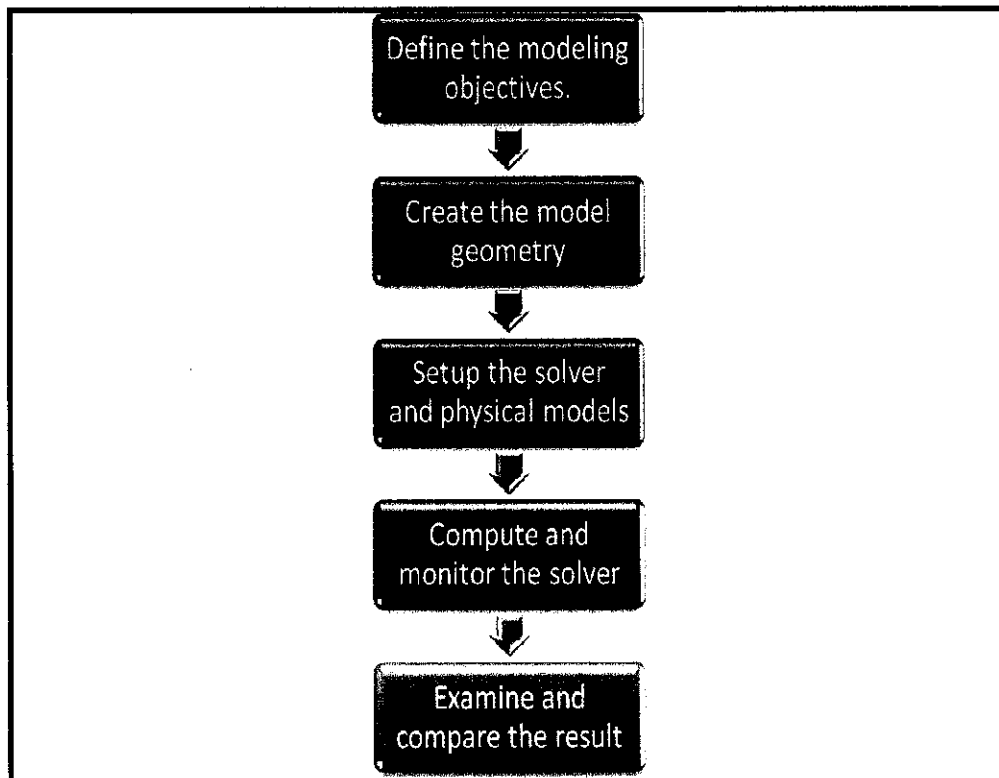


Figure 9: Research Methodology

### 3.2.1 *Define the modeling objectives*

The objective of this modeling is to study the effect of velocity changes on LDL accumulation and to investigate the effect of LDL sizes that corresponding to LDL accumulation. Thus, the parameter that needs to be controlled is the inlet velocity of the model.

### 3.2.2 *Create model geometry*

In the pre-processing, solid geometry is modeled. In this case, geometry with stenosis tube creates in the ANSYS package. The model created has the 22 mm length and 2 mm diameter. This 3D model is in a position at X-axis for flow direction.

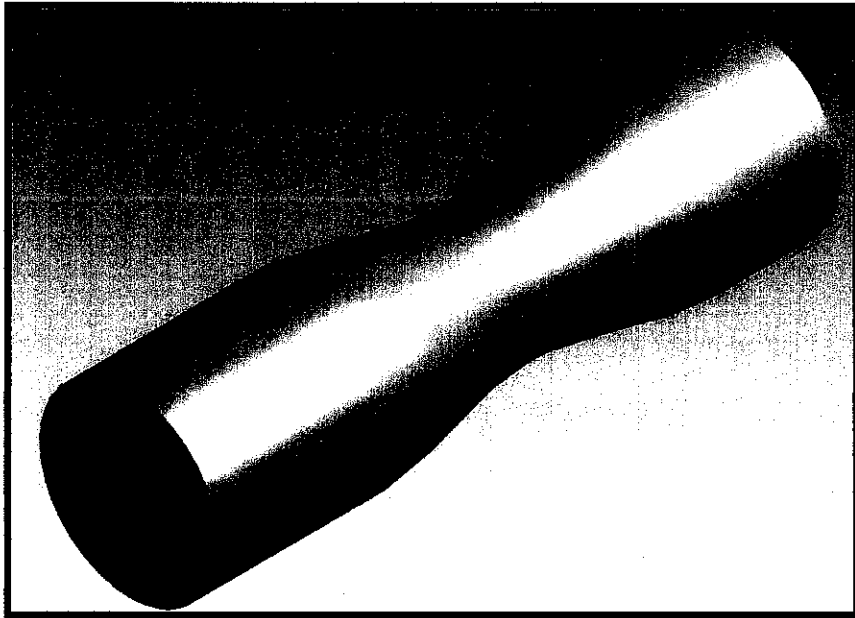


Figure 10: Diseased Artery Geometry

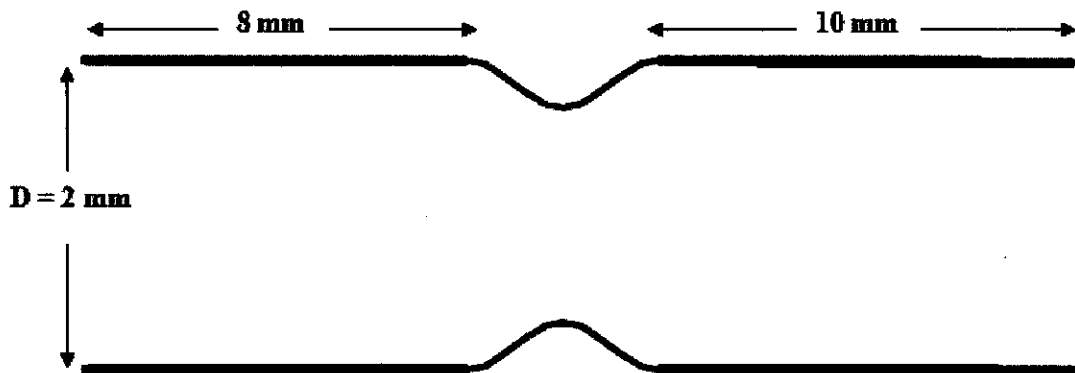


Figure 11: Normalised Scale

### ***3.2.3 Meshing.***

Mesh is generated with quadrilateral mesh structures as its finite control volume. The figure below shows the stenosis geometry with mesh.

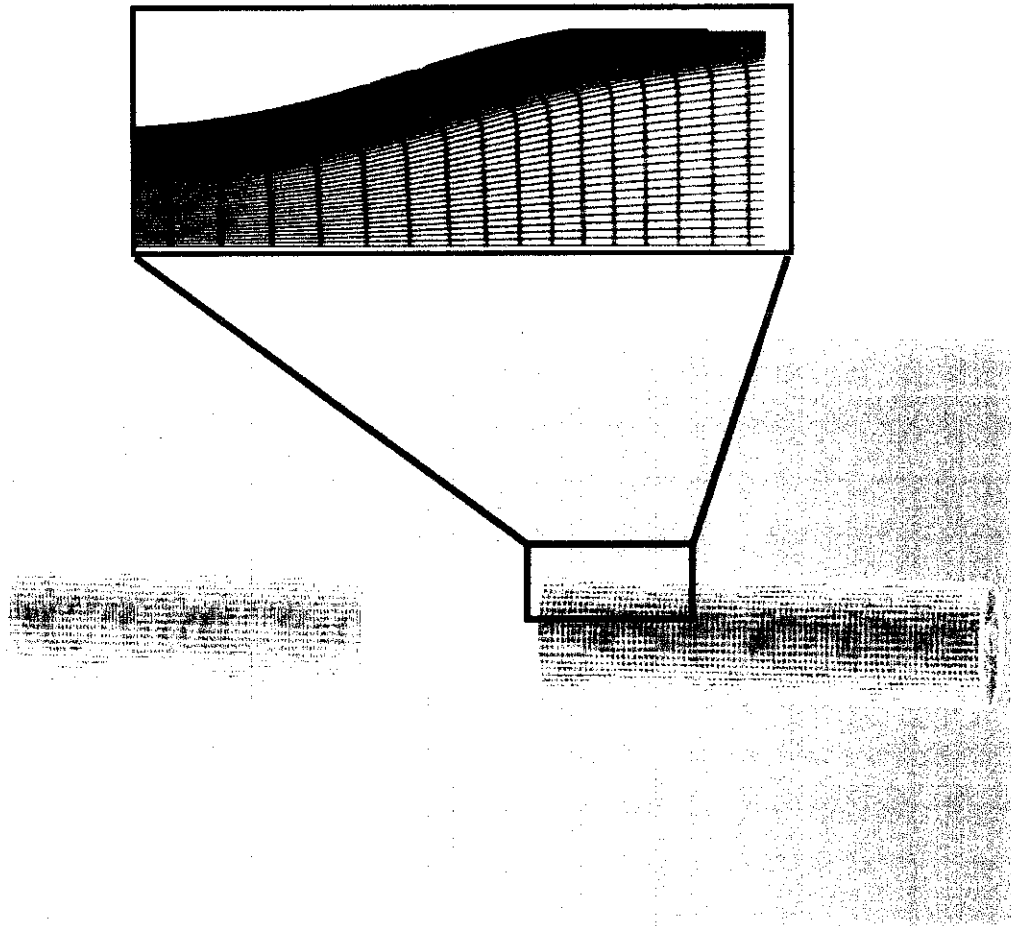


Figure 12: Quadrilateral grid mesh.

Figure above shows the interface on how to start modeling the geometry. Basically, the design can be launched in a standalone mode (component system) in a workbench or straight away specify the system that will be used to solve the geometry. For analysis systems, the sequence on simulation has been defined. After finishing with design modeling, mesh can be generated. The computational grid consists of 464437 cells, 475661 nodes and 1404111 faces.

### ***3.2.4 Setup the solver and physical models***

As explained in the earlier section, FLUENT needs a user to set up the numerical model. The data such as boundary condition, blood flow condition and appropriate

physical model. In this case, the change of energy is negligible since human body has a constant body temperature around 37°C. For the parameter controlled which is inlet velocity, it will subject to the normal human cardiac cycle as shown below.

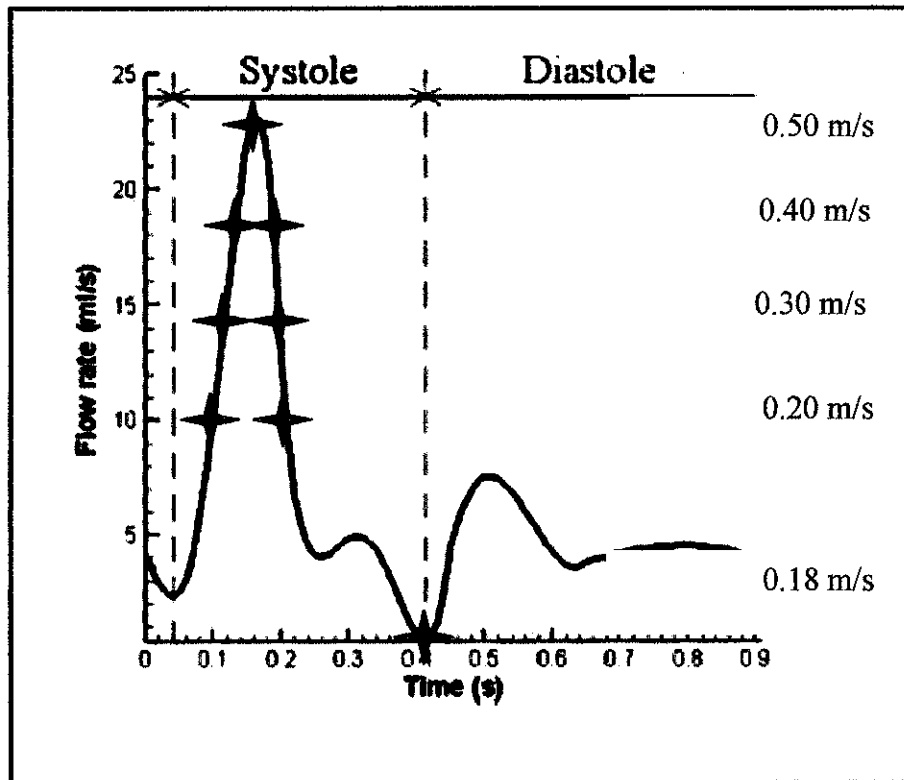


Figure 13: Normal Cardiac Cycle

The data as stated below will be used as input during simulation.

- **Physical models**

- **Viscous model**

- Spalart allmaras
    - Discrete phase

- **Material properties of blood**

Density	1060 kg/m <sup>3</sup>
Viscosity	0.001 kg/m.s

- **Material properties of LDL**

Density	1050 kg/m <sup>3</sup> (Keith, 1993 )
---------	---------------------------------------

- **Boundary conditions**

Inlet velocity	0.18m/s, 0.2m/s, 0.4 m/s, 0.5m/s
----------------	----------------------------------

- **Solution Methods**

Pressure velocity coupling	SIMPLEC
Pressure	Standard
Momentum	Second Order Upwind
Modified Turbulent Viscosity	2 <sup>nd</sup> Order Upwind

After inserting all the required data into the solver settings, the discrete domain which is in grid was solved by the conservation equations until a convergence is reached. This convergence will subject to the error level set by the user.

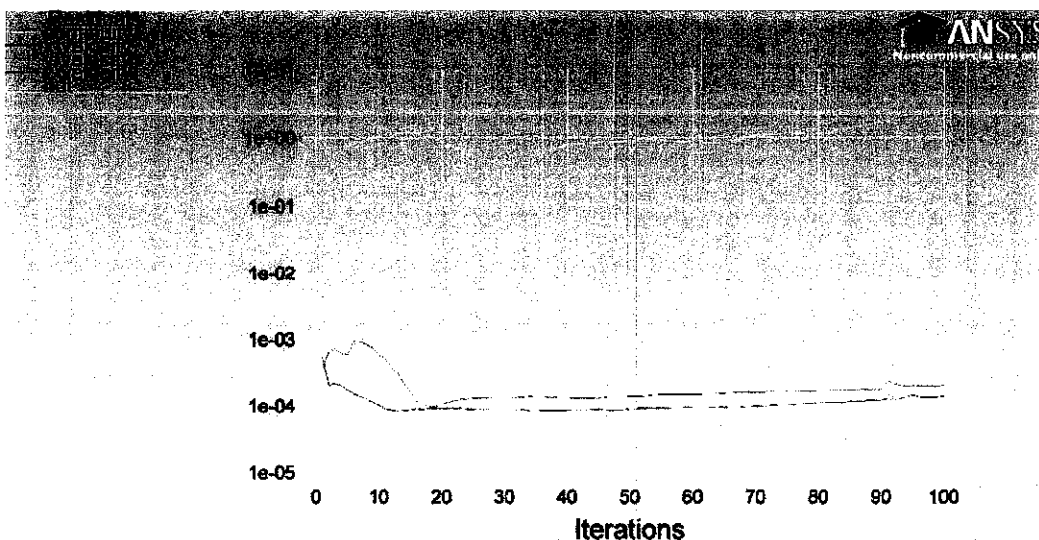


Figure 14: Scaled Residual

The solutions converged when the changes in solution variables from iterations to the next iterations are negligible. Figure 15 provides the mechanism to monitor the simulation trends.

### **3.3 Project Milestone**

The figure below shows the project timeline for “Accumulation of Low Density Lipoprotein in Diseased Artery”. The project is started with finding and collecting the previous research paper that related to the project. About 5 weeks is allocated for this paper study, 1 week on the atherosclerosis study including the survey, 2 weeks on analysing the research paper on mass transfer of lipid and methodology used such as the understanding on how CFD works also about the properties required for solver as mentioned earlier. As a beginner, ANSYS training will be held in order to introduce the ANSYS feature and other things such as building the geometry. The modelling starts on the following week and onward until the end of the FYP2.

By referring to Figure 15, it shows the expected milestone, which is prepared before the project is started and also the actual milestone, which is prepared after the project is about to complete. Therefore, the project milestone can be seen clearly either it is finished on time.

No	Detail/Week	1	2	3	4	5	6	7	8	9	10	11	12	13	14
1	Atherosclerosis study														
2	Mass Transfer of LDL														
3	Methodology study														
4	ANSYS FLUENT Familiarization														
5	ANSYS FLUENT Training														
6	Design the modeler, meshing														
7	Setup the solver														
	Run Case 1														
	Run Case 2														
8	Technical Paper Submission														
	VIVA and presentation														


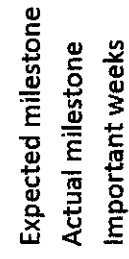
 Expected milestone  
 Actual milestone  
 Important weeks

Figure 15: Project Milestone



## CHAPTER 4

### RESULT AND DISCUSSION

The recirculation region on downstream of restriction area of chosen velocities is shown in this chapter. Each velocity is analyzed based on the contour and vector of velocity magnitude and residence time of LDL particle.

#### 4.1 Flow Movement at Inlet Velocity 0.18 m/s

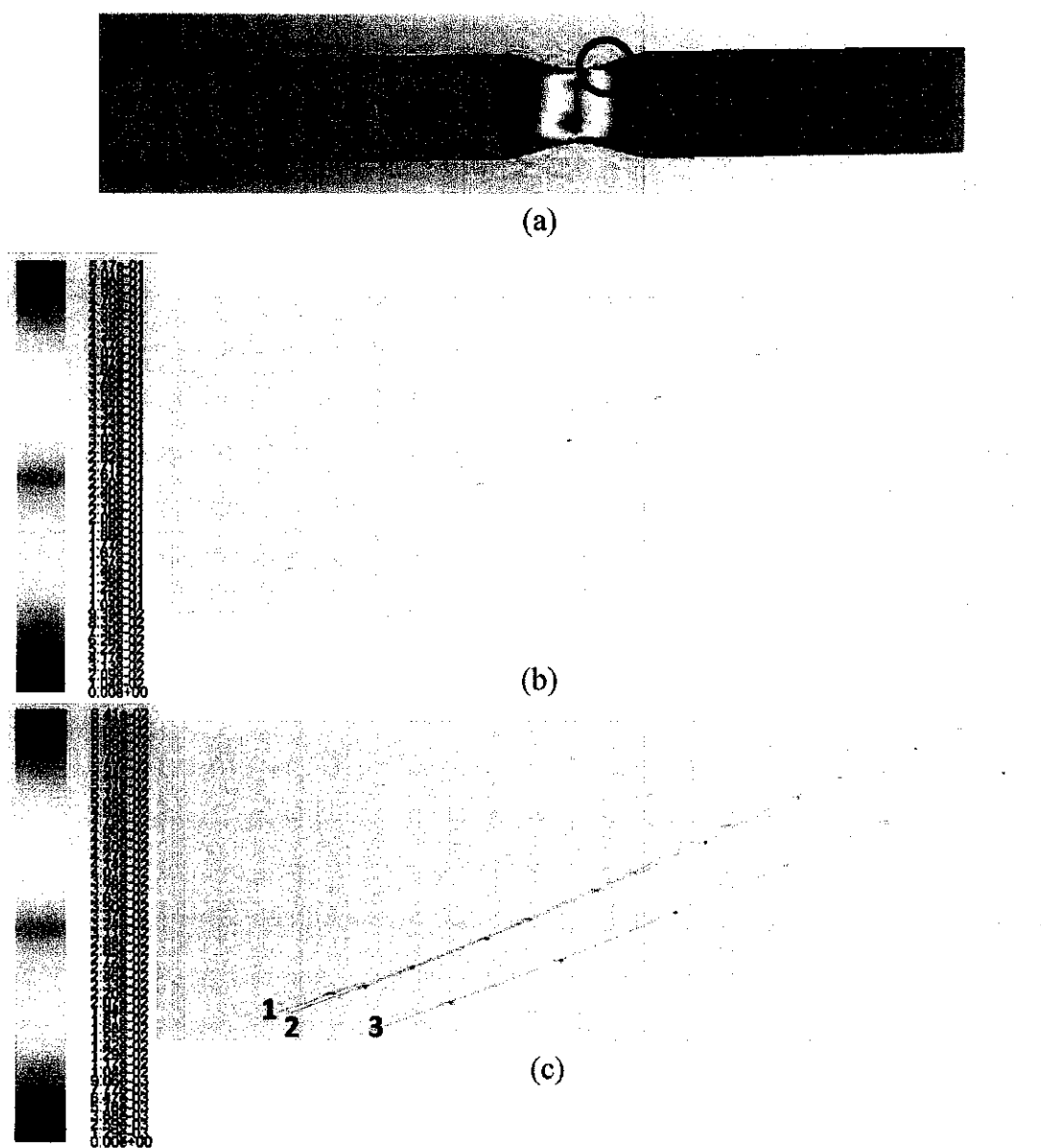


Figure 16: Velocity (a) contour (b) vector (c) LDL residence time at inlet velocity 0.18 m/s

Based on figure 16 (a) shows a velocity contour of inlet velocity 0.18 m/s. All velocities are increasing but decreasing toward the wall of the tube. The change of velocity from lowest velocity, 0.00104 m/s where is near the wall to the velocity about 0.198 m/s at the middle of the tube along upstream of restriction area. When the flow is approached the restriction area, the velocity become higher, 0.250 m/s (indicate by green color gradient) and it gradually increased to the highest velocity, 0.517 m/s at the middle of the restriction area.

While figure 16 (b) shows the velocity vector at inlet velocity 0.18 m/s. The aim of this study was to investigate the recirculation region at downstream of restriction area. The recirculation region is indicated by red circle in figure 17 (a). The closer fluid with respect to the wall, the color become darker and the length of vector arrow become shorter. It is where the velocity is the lowest, 0.00143 m/s. From vector arrow, it shows that there is no recirculation region occurs. From both figures (a and b) it can be said that, flow for inlet velocity 0.18 m/s is a laminar. The inlet Re number is calculated and it equals to 94.5.

In order to study the cause of LDL, the study is focusing on the positions near to the wall. This is because, as it near to the wall, wall shear stress (WSS) will be decreased. The decreasing of WSS is corresponding to the residence time. The longer residence time of LDL particle, the higher chances of LDL diffusion into the artery wall.

In figure 16 (c) the residence times of three LDL particles at three different positions are analyzed. The three LDL particles are indicated by different positions near to the tube wall. Position 1 is the closest position to the tube wall at  $x= 0.4$  mm,  $y= 0$  mm,  $z= -0.71$  mm. While the line in middle is in the position  $x= 0.4$  mm,  $y= 0$  mm,  $z= -0.7$  mm (position 2) and the third line in the position  $x= 0.4$  mm,  $y= 0$  mm and  $z= -0.6$  mm (position 3). The LDL particles residence time in these three positions show same residence time approximately 0.00129 seconds which is indicates by color of line. Lipid residence time is studied in concerning that the longer lipid stay on artery wall, the chance for diffusion into artery wall is high.

## 4.2 Flow Movement at Inlet Velocity 0.20 m/s

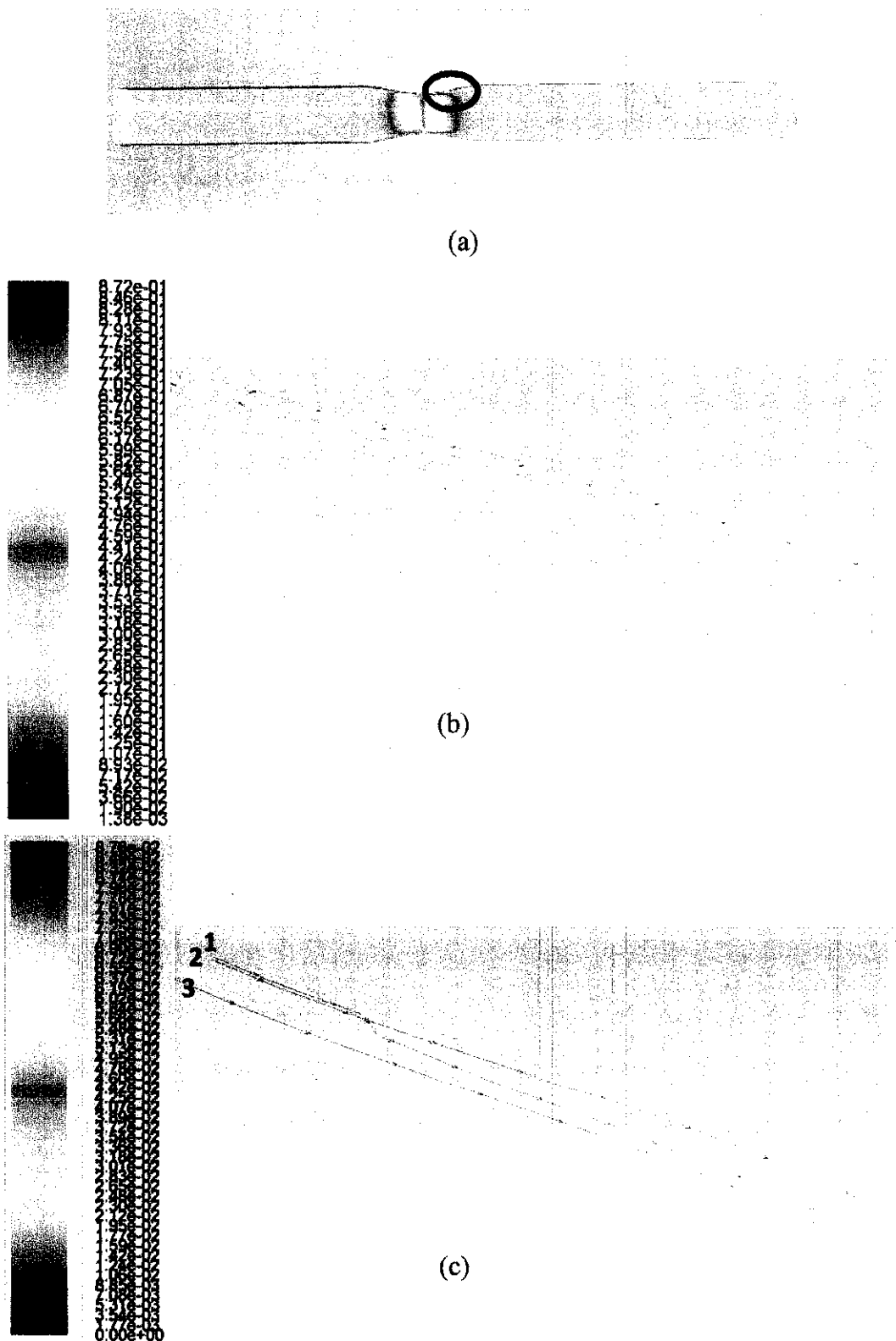


Figure 17: Velocity (a) contour (b) vector (c) LDL residence time at inlet velocity 0.2 m/s

Based on figure 17 (a), high velocity region is created at upstream of restriction area. All velocities are increasing but decreasing toward the wall of the tube. The change of velocity from lowest velocity, 0.00138 m/s where is near the wall to the velocity about 0.248 m/s at the middle of the tube. When the flow is approached the restriction area, the velocity become more higher, 0.547 m/s and it gradually increased to the highest velocity, 0.872 m/s at the middle of the restriction area.

Figure 17 (b) represents the velocity after restriction area. Dark and short vector arrow indicates the condition near the wall of artery where velocity is the lowest, 0.00138 m/s at that region. Same as previous study, at inlet velocity 0.20 m/s there is no recirculation region occurs here. It can be determined by backflow arrows. From both figures (a and b) it can be said that, flow for inlet velocity 0.20 m/s is a laminar. The inlet Re number is calculated and it equals to 105.

In figure 17 (c), the LDL particles in these three positions (same as previous study) show same residence time approximately 0.00177 seconds. Therefore, the chance of LDL accumulation in this region is lowered as it is laminar flow and no recirculation region at downstream of restriction area.

By comparing the residence time at inlet velocity 0.18 m/s with 0.20 m/s, the particles move faster compare to previous case study. As mentioned earlier, recirculation region does not exist in both case studies, velocity at 0.18 m/s and 0.20 m/s.

### 4.3 Flow Movement at Inlet Velocity 0.30 m/s

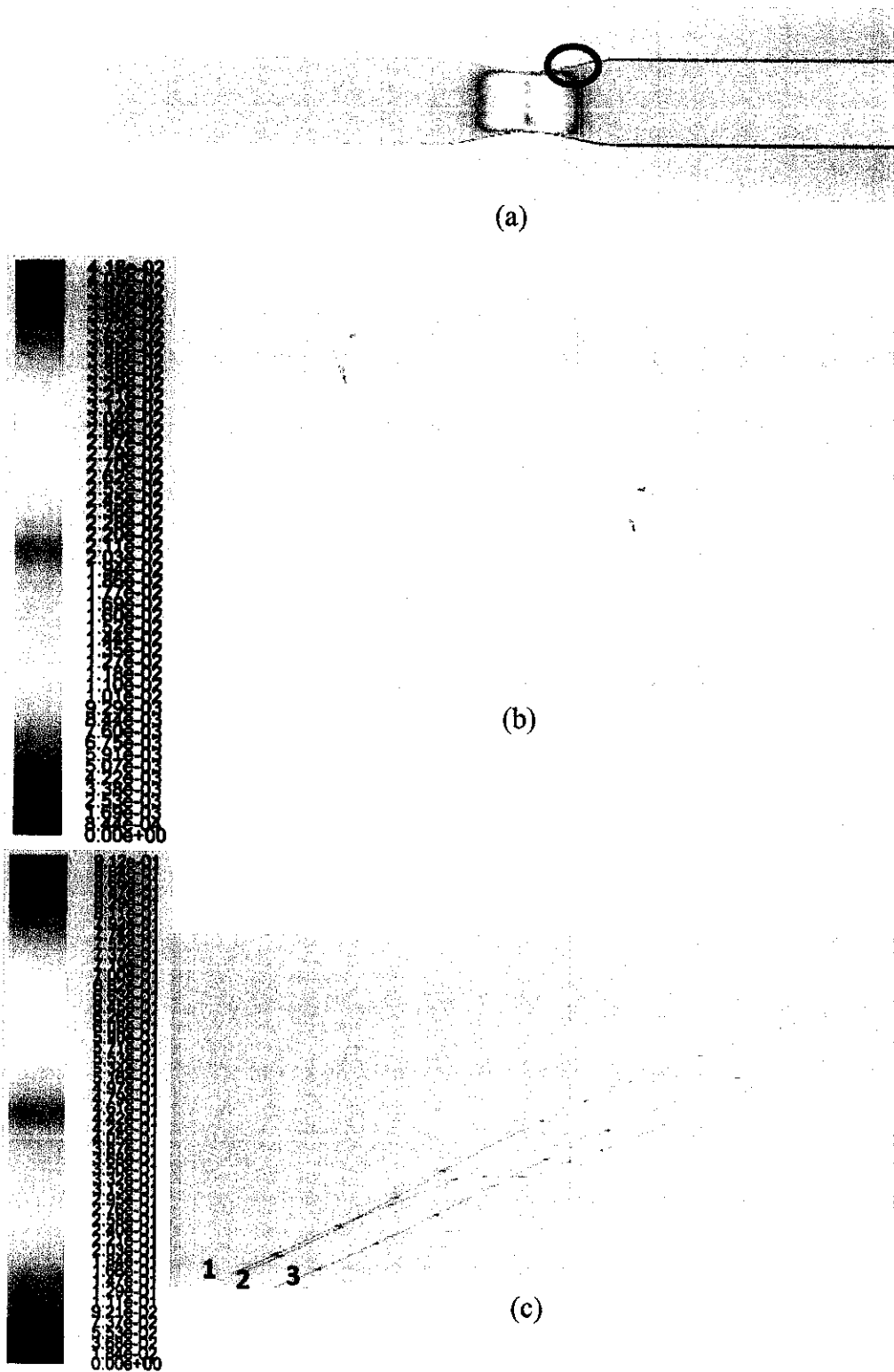


Figure 18: Velocity (a) contour (b) vector (c) LDL residence time at inlet velocity 0.3 m/s

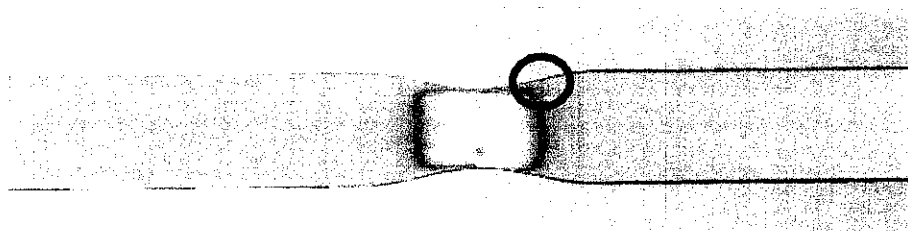
Based on figure 18, high velocity region is created at upstream of restriction area. All velocities are increasing but decreasing toward the wall of the tube. The change of velocity from lowest velocity, 0.0184 m/s where is near the wall to the velocity about 0.240 m/s at the middle of the tube. When the flow is approached the restriction area, the velocity become more higher, 0.416 m/s and it gradually increased to the highest velocity, 0.866 m/s at the middle of the restriction area.

Velocity vector in figure 18 (b) is showing the velocity vector at red circle region (figure 18 (a)). The closer fluid with respect to the wall, the color become darker and the length of vector arrow become shorter. The arrow also indicates the velocity of the flow. Shorter the arrow indicates shorter time it stays at the region. The velocity is about 0.018 m/s which are near to zero and recirculation region occurs. The backflow arrow with darker color is indicated the recirculation region. Even though the inlet Re number, 157.5 is still considering as laminar flow because the recirculation region not only occur for turbulent flow but it also can occur for laminar flow.

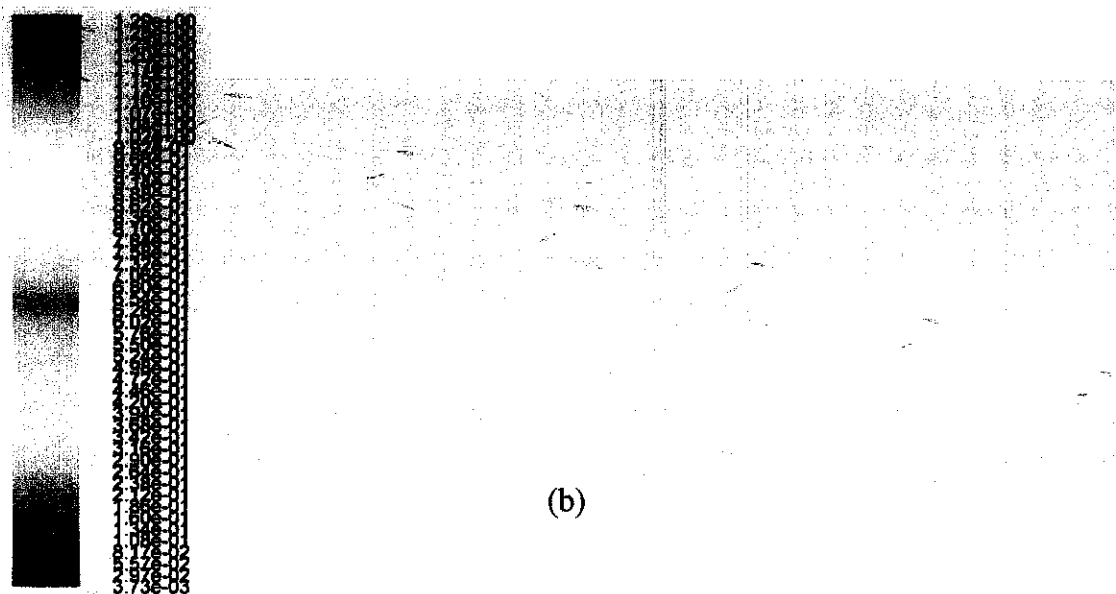
Figure 18 (c) shows the LDL residence time at inlet velocity 0.3 m/s. The lipid particles in these three positions show same residence time approximately 0.00884 seconds. LDL particle in position 1 migrates away from the wall but it has same residence time and velocity. For LDL in position 2, it suddenly migrates near to the wall. Position 3 is different about 0.1 mm from position 2 and it shows that the movement of LDL particle is smooth compare to two positions earlier.

By comparing this study with two previous studies, the movements of these particle LDL do not show a straight line. This is due to constriction in recirculation region.

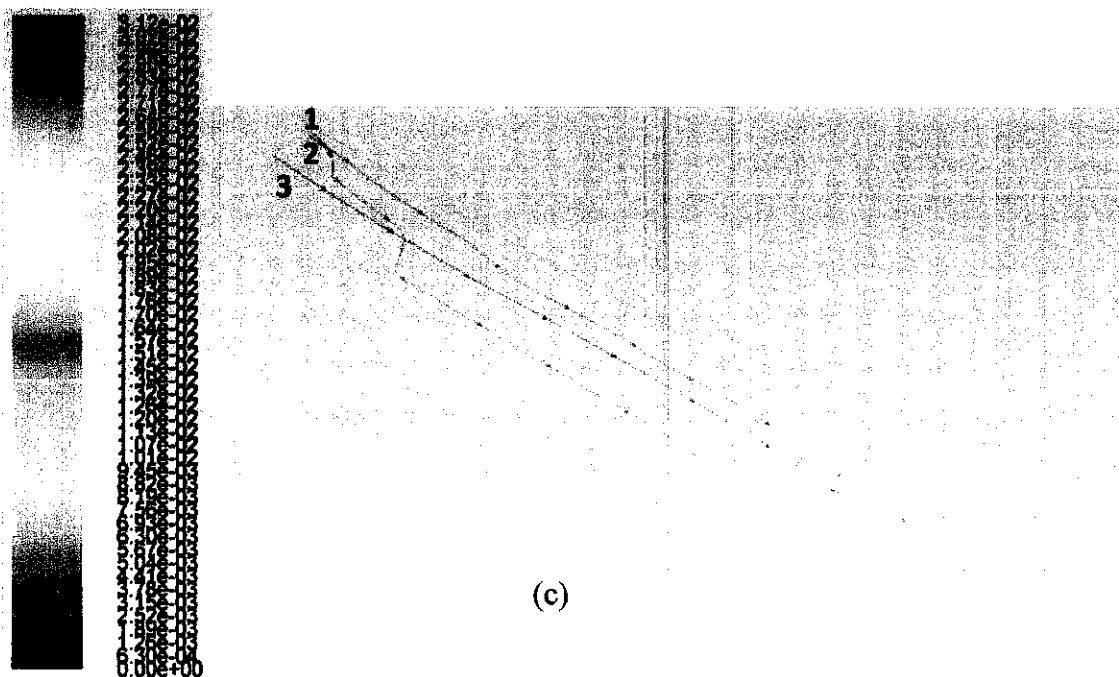
#### 4.4 Flow Movement at Inlet Velocity 0.40 m/s



(a)



(b)



(c)

Figure 19: Velocity (a) contour (b) vector (c) LDL residence time at inlet velocity 0.4 m/s

Based on figure 19 (a), high velocity region is created at upstream of restriction area. All velocities are increasing but decreasing toward the wall of the tube. The change of velocity from lowest velocity, 0.00373 m/s where is near the wall to the velocity about 0.394 m/s at the middle of the tube. When the flow is approached the restriction area, the velocity become more higher, 0.680 m/s and it gradually increased to the highest velocity, 1.25 m/s at the middle of the restriction area.

From figure 19 (b), it shows that the recirculation region occur at inlet velocity 0.4 m/s. However, the velocity near the wall is about 0.342 m/s higher than at inlet velocity 0.3 m/s which is 0.276 m/s. It can be said that the recirculation region at inlet velocity 0.4 m/s has bigger recirculation region compare to recirculation region at inlet velocity 0.3 m/s. However, need to be reminded that, both conditions still having the inlet Re number in the range of laminar flow, thus the recirculation region will not big as turbulent flow. The inlet Re number at inlet velocity 0.4 m/s is 210.

Based on figure 19 (c), the LDL particles in these three positions show same residence time approximately 0.00252 seconds. Lipid particle position 1 moves away from the wall but with the same residence time and velocity. For LDL in position 2, travel in a straight manner toward the outlet and same goes to lipid in position 3.

By comparing this study with previous studies, LDL particles with this velocity have highest residence time at recirculation region. Therefore, the chance of LDL accumulation at this region with velocity 0.4 m/s is high.



#### 4.5 Flow Movement at Inlet Velocity 0.50 m/s

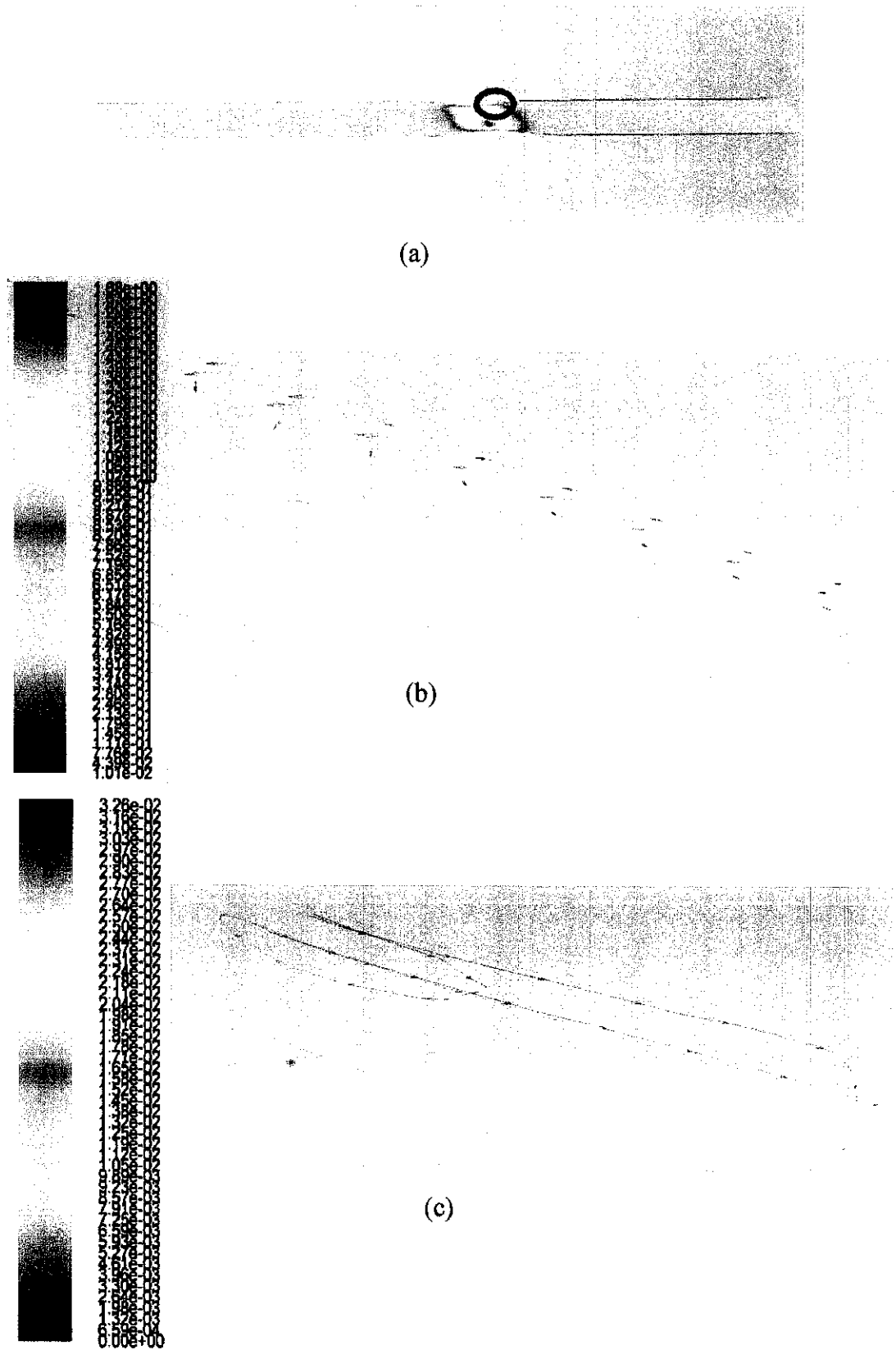


Figure 20: Velocity (a) contour (b) vector (c) LDL residence time at inlet velocity 0.5 m/s

Based on figure 20 (a), it shows the velocity magnitude of velocity 0.5 m/s. The flow patterns show the same as at three inlet velocities earlier. The velocity magnitude at the inlet has the same velocity from the middle of the tube to tube wall which is about 0.550 m/s. The velocity keeps increasing when the flow is approaching the restriction area. It started to increase from 0.820 m/s to 1.68 m/s when it reached the 30% reduction area of stenosis. At the downstream of restriction area, the velocity magnitude started to decrease significantly from 1.19 m/s to 0.617 m/s. The lowest velocity magnitude where is 0.0101 m/s situated near to the wall.

From figure 20 (b) it represents the velocity vector of 0.5 m/s at the respective region which indicates by red circle in figure 26 (a). The velocity near to the wall has the lowest velocity and it is created backflow. This backflow will produce the small vortex after restriction area and also known as recirculation region. The inlet Re number at inlet velocity 0.5 m/s is 262.5.

By referring to figure 20 (c), the LDL particles in these three positions show same residence time approximately 0.00132 seconds. LDL particle motion of this study shows some differences compare to three previous studies. Position 1 with residence time 0.0033 seconds moves away from the wall and creates backflow at the position near to position 3. Then, it travels back to the outlet of tube. It same goes to lipid in position 2. It creates backflow quite far from wall and postion 3. The residence time of the LDL increase from 0.0033 seconds to 0.0326 seconds. Thus, it has higher chance to diffuse into the artery wall and form plaque in artery wall. Meanwhile, the LDL in position 3 flows straight and did not cause any backflow. This pattern of LDL movements is different from three inlet velocity earlier. It might occur due to high vorticity at downstream of restriction area.

At each inlet velocity, the blood flow show the same pattern as the velocity is getting higher toward the middle of the tube. Therefore, it obeys the Hagen Poiseuille theory as it creates the parabolic velocity profile. In addition, at each velocity, the highest velocity occurs at the middle restriction area. This is because; when the flow travels towards the reduction surface area it will cause a reduction in fluid pressure as well. As a sequence of pressure reduction, fluid velocity will increase in order to satisfy the equation of continuity.

Before analyzing the residence time of LDL, the blood flow pattern need to be studied. From the inlet Re number calculation, it shows all blood flow in all velocities are laminar. The blood flow at inlet velocity 0.3 m/s, 0.4 m/s and 0.5 m/s show the formation of recirculation region at downstream of restriction area.

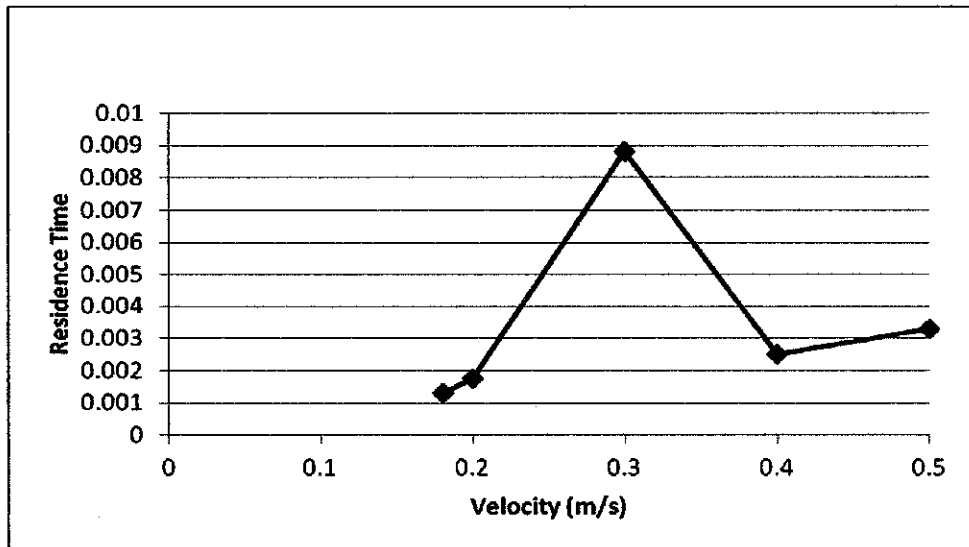


Figure 21: Graph of velocity versus residence time at recirculation region.

As the study is to compare the residence time at the recirculation region only, here is shows the residence time of LDL at recirculation region. By analyzing the residence time at all velocities, the LDL particle at velocity 0.18 m/s has shortest time at downstream of restriction area, 0.00129 seconds. The pattern of residence time keeps increasing with the increasing of velocity. For velocity 0.2 m/s, the residence time is about 0.00177 seconds. The residence time of velocity 0.3 m/s is the highest one, 0.00884 seconds and it does not show the right track of residence time because residence time at 0.4 m/s and 0.5 m/s are 0.00252 seconds and 0.00330 seconds, respectively. It has a thought that, at inlet velocity 0.3 m/s, it creates high vorticity compare to inlet velocity 0.4 m/s and 0.5 m/s. However, the LDL at these three velocities keeps longer at expected area as it create recirculation region.

From the Hagen Poiseuille theory, the velocity will be decreased when it is approaching the wall and it will create the parabolic velocity profile. The value of the velocity near the wall allows the evaluation of wall shear stress (WSS) values. Generally, WSS is proportional with the velocity gradient. Lower the velocity, WSS will be lowered too and it takes longer residence time of LDL particle.

#### 4.6 The Study of Lipid Size Variation in Corresponding To Lipid Accumulation.

The study has been simulated with different sizes of lipid which are 1  $\mu\text{m}$ , 3  $\mu\text{m}$  and 5  $\mu\text{m}$ . Three colors indicate three different diameters. Red line (particle 1) indicates the lipid diameter 1  $\mu\text{m}$  while white line (particle 2) indicates the lipid with diameter 3  $\mu\text{m}$  and green line (particle 3) indicates the lipid with 5  $\mu\text{m}$ . This study is observed at one constant position  $x= 0.4 \text{ mm}$ ,  $y= 0 \text{ mm}$ ,  $z= -0.71$ . The data is extracted from the XY plot of path length (mm) versus particle residence time in appendix C1.

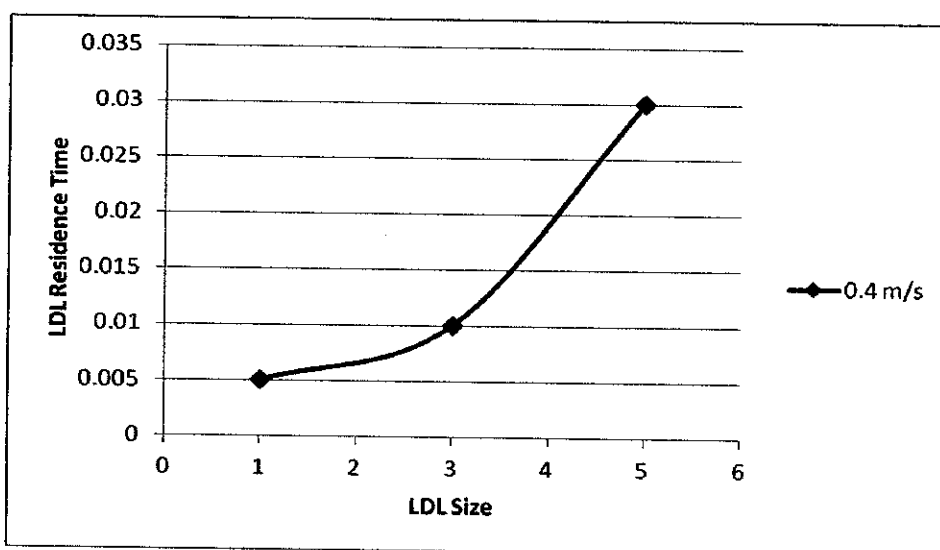


Figure 22: Graph of LDL size versus LDL residence time at inlet velocity 0.4 m/s

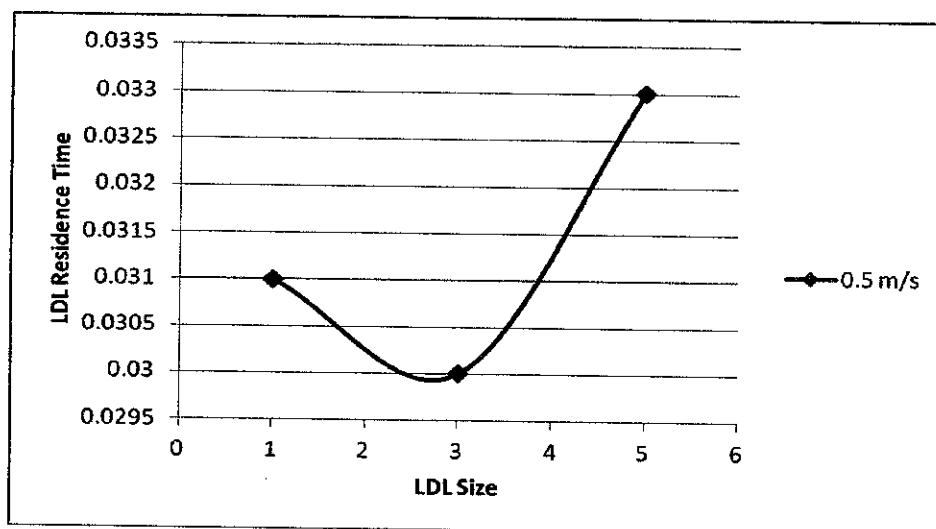


Figure 23: Graph of LDL size versus LDL residence time at inlet velocity at 0.5 m/s

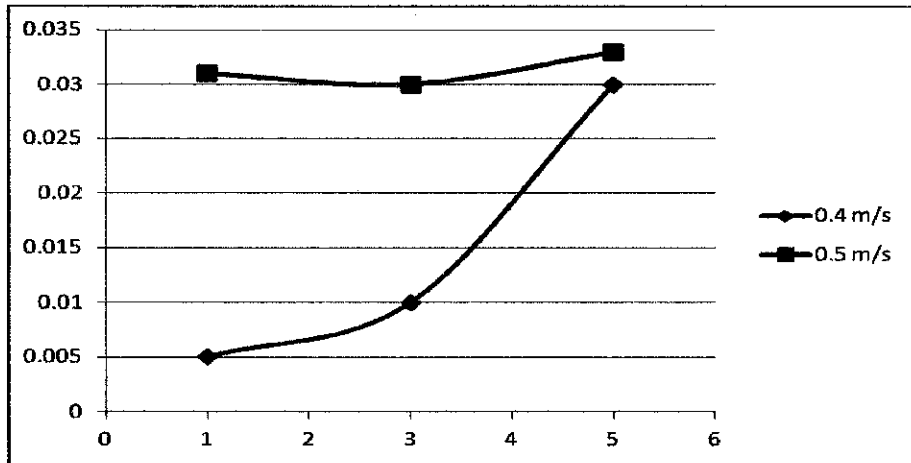


Figure 24: LDL size versus LDL residence time at two velocities

From figure 22 it shows the graphs of LDL size versus LDL residence time at 0.4 m/s. It shows that smallest particle, 1  $\mu\text{m}$  has the smallest residence time, 0.005 seconds. The LDL residence time it increases gradually with the LDL size.

Figure 23 shows the graphs of LDL size versus LDL residence time at 0.5 m/s. It shows that smallest particle, 1  $\mu\text{m}$  has the shortest residence time, 0.031 seconds. The LDL residence time for 3  $\mu\text{m}$  diameter of LDL shows small decrement in its residence time as 0.03 seconds. This graph does not increase gradually as Figure 22. This is because for 5  $\mu\text{m}$ , its residence time shows some increment which is 0.031 seconds.

While figure 24 shows the comparison of LDL size versus LDL residence time at two inlet velocities, 0.4 m/s and 0.5 m/s. It shows that inlet velocity at 0.5 m/s has longer residence time compare to inlet velocity at 0.4 m/s.

As the LDL size becomes bigger, drag force of LDL particle will increase. Therefore, the particle inertia of LDL also increases. Bigger size of LDL will have bigger momentum and vice versa. bigger momentum lead to low velocity and that is the reason why bigger size of LDL stay longer at area of study compare to small particle.

## **CHAPTER 5**

### **CONCLUSIONS & RECOMMENDATIONS**

#### **5.1 Conclusion**

For blood flow behavior at different inlet velocity, it is observed that it has the same pattern of blood flow in upstream of restriction area. However, the increment in velocity has caused the recirculation region at downstream of restriction area. The characteristic of blood flow can be determined from inlet Reynolds (Re) number. From Re number, it shows that as the inlet velocity increased, the Re number increased as well. Thus, it describes the formation of recirculation region.

Then, the LDL residence time at recirculation region is studied. From the result obtained, the LDL particles move smoothly at lower inlet velocity as it does not have recirculation region. However, uncertainty had occurred at inlet velocity 0.3 m/s as the residence time increased drastically before decreasing at inlet 0.4 m/s. It might be due to high vorticity at recirculation region.

Consideration of LDL size in accumulation of LDL near wall of tube shows that large LDL size will have longer residence time in artery wall as illustrated by figure 22 and 23. Over years, it will cause the plaque and become danger as it can cause CVD.

As the conclusion, the high velocity will create a recirculation region. When it has the recirculation region, the LDL particle will stay longer at the recirculation region. Thus, residence time has contributed to the formation of plaque by LDL. Secondly, LDL sizes also related powerfully to the atherosclerosis progression.

## 5.2 Recommendations

In a future study, the analysis should be done by analyzing more different sizes for the study of LDL size variation to get more significant result.

The studies can be done in order to see the extension of LDL particle on the mass transfer of LDL in porous medium. Three types of models have been clarified corresponding to the arterial wall study, wall free models, single layered models and multi layered models. The wall free models are the simplest model and have been used to model solute dynamics in the lumen for oxygen, albumin, and LDL. In these cases, arterial wall is treated as a boundary condition, thus the transport process does not take into account. Meanwhile, for single layered models arterial wall acts as one layer of porous media by taking into account the homogeneous transport properties. It has been employed to model oxygen and LDL transport. Lastly, multi layered model treats arterial wall as the layers of porous medium with different transport properties and has been the most comprehensive models (Sun. N et.al, 2006).

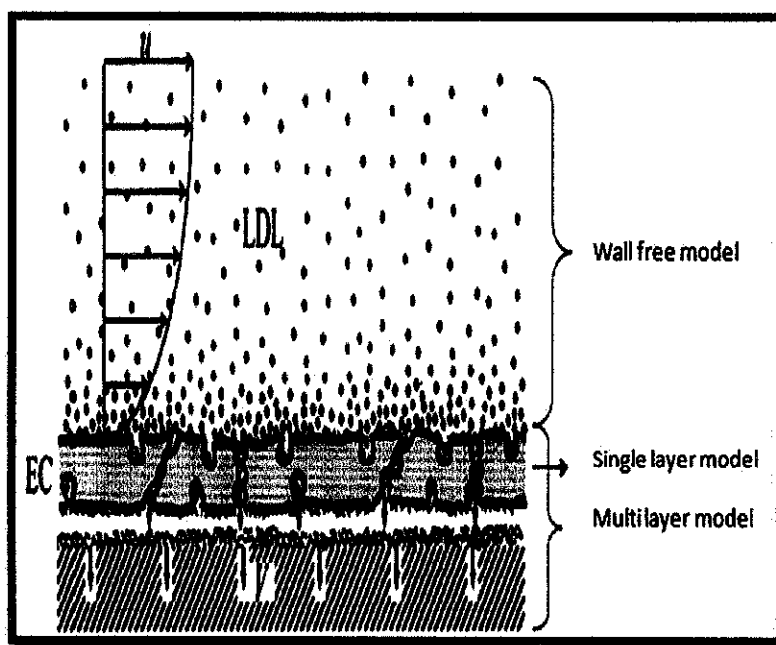


Figure 25: Types of Computational Modelling of Porous Media

Another recommendation is about studying on estimation time dependent growth function for thickness of the arterial wall. This is because the growth rate of the plaques is not linear with time and the fact that the rate is fluctuated against time. In

order to model this study, more data especially on genetic condition, age of individuals, physiological properties need to be collected.



## REFERENCES

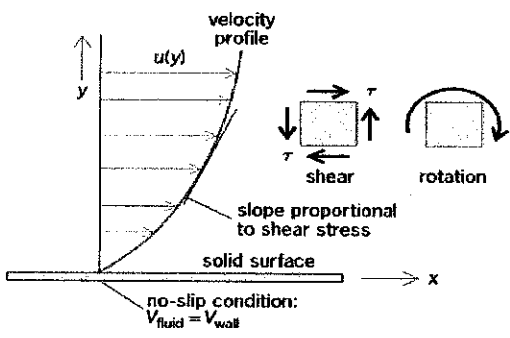
- Bird, R. B. (2002). The equations of change for isothermal systems . In *Transport phenomena* (2nd edition ed., pp. 98-98). New York: John Wiley.
- Cardiovascular diseases (CVDs)*. (2011). Retrieved February 10, 2012, from <http://www.who.int/mediacentre/factsheets/fs317/en/>
- Chakravarty, S., Mandal, P. K., & Andersson, H. I. (2009). Mass transfer to blood flowing through arterial stenosis. *Zeitschrift Für Angewandte Mathematik Und Physik (ZAMP)*, 60(2), 299-323.
- Chapter 2, Law of Poiseuille. Retrieved July 6, 2012 from <http://www.buchhandel.de/WebApi1/GetMmo.asp?MmoId=999524&mmoType=PDF&isbn=9780387233451>
- Ethier, C. R. (2002). Computational modeling of mass transfer and links to atherosclerosis. *Annals of Biomedical Engineering*, 30(4), 461-471.
- Fournier, R. L. (2011). *Basic transport phenomena in biomedical engineering* CRC Press.
- Hooi, C. G. (2012). *Predicting heart disease risks*. Retrieved February 8, 2012, from <http://thestar.com.my/health/story.asp?file=/2012/2/5/health/10665267&sec=health>
- Ikbal, M. A., Chakravarty, S., & Mandal, P. (2010). Numerical simulation of mass transfer to micropolar fluid flow past a stenosed artery. *International Journal for Numerical Methods in Fluids*,

- Kaazempur-Mofrad, M., Wada, S., Myers, J., & Ethier, C. (2005). Mass transport and fluid flow in stenotic arteries: Axisymmetric and asymmetric models. *International Journal of Heat and Mass Transfer*, 48(21), 4510-4517.
- Katrtsis, D., Kaiktsis, L., Chaniotis, A., Pantos, J., Efstathopoulos, E. P., & Marmarelis, V. (2007). Wall shear stress: Theoretical considerations and methods of measurement. *Progress in Cardiovascular Diseases*, 49(5), 307-329.
- Keith U.I, Vincent W.B, Stocker R & Walling C (1993). Autoxidation of lipids and antioxidation by  $\alpha$ -tocopherol and ubiquinol in homogeneous solution and in aqueous dispersions of lipids: Unrecognized consequences of lipid particle size as exemplified by oxidation of human low density lipoprotein. *Proc. Natl. Acad. Sci. USA*, 90, 45-49.
- Lantz, J., & Karlsson, M. (2012). Large eddy simulation of LDL surface concentration in a subject specific human aorta. *Journal of Biomechanics*, 45(3), 537-542.
- Rizzo M & Bernies K. (2006). Low-density lipoprotein size and cardiovascular risk assessment. Oxford University Press on behalf of the Association of Physics
- Sacks F.M. & Campos H (2003). Low Density Lipoprotein Size and Cardiovascular Disease: A Reappraisal. *The Journal of Clinical Endocrinology & Metabolism* 88(10):4525–4532
- Shuib A et al (2012), Flow Regime Characterization in a Diseased Artery Model. *International Journal of Biological and Life Sciences*, 8:4, 234-238

- Sun, N., Wood, N. B., Hughes, A. D., Thom, S. A. M., & Xu, X. Y. (2007a). Influence of pulsatile flow on LDL transport in the arterial wall. *Annals of Biomedical Engineering*, 35(10), 1782-1790.
- Sun, N., Wood, N. B., Hughes, A. D., Thom, S. A. M., & Yun Xu, X. (2007b). Effects of transmural pressure and wall shear stress on LDL accumulation in the arterial wall: A numerical study using a multilayered model. *American Journal of Physiology-Heart and Circulatory Physiology*, 292(6), H3148-H3157.
- Superko HR & Gadesam RR (2008). Is it LDL particle size or number that correlates with risk for cardiovascular disease? *Curr Atheroscler Rep* 10, 377-385.
- Varady K.A et. al (2010), Improvement in LDL particle size and distribution by short term alternate day modified fasting in obese adults. *British Journal of Nutrition*, 105,580-583

## APPENDICES

### A1) GLOSSARY

TERM	DEFINITION
Reynolds number, $Re$	An indication of the relative importance of inertial and viscous forces in the fluid system. (Bird, 2002) $Re = \frac{\rho v L}{\mu}$ Where: $v$ = the mean velocity of the object relative to the fluid (m/s) $L$ = characteristic linear dimension (m) $\mu$ = is the dynamic viscosity of the fluid (Pa·s or N·s/m <sup>2</sup> or kg/ (m·s)) $\rho$ = density of the fluid (kg/m <sup>3</sup> )
Shear stress, $\tau$	Force per unit area (F/A) that is exerted by the flowing fluid on the surface of the tube (Katritsis et al., 2007)
Shear rate, $\gamma$	velocity gradient, (dv/dx) <div style="text-align: center; margin: 10px 0;">  </div> (White, 2008)

## B1) DERIVATION OF NAVIER STOKES EQUATION

### The Navier-Stokes Equations

Adam Powell

May 7, 2004

Below are the Navier-Stokes equations and Newtonian shear stress constitutive equations in vector form, and fully expanded for cartesian, cylindrical and spherical coordinates. The momentum equation is given both in terms of shear stress, and in the simplified form valid for incompressible Newtonian fluids with uniform viscosity.

**Vector Form** These are the equations written using compact vector notation.

The continuity equation (conservation of mass):

$$\frac{D\rho}{Dt} + \rho \nabla \cdot \vec{u} = 0 \quad (1)$$

The motion equation (conservation of momentum):

$$\rho \frac{D\vec{u}}{Dt} = -\nabla p - \nabla \cdot \tau + \rho \vec{g} \quad (2)$$

Shear stress constitutive equation:

$$\tau = -\mu \left( \nabla \vec{u} + \nabla \vec{u}^T - \frac{2}{3} \nabla \cdot \vec{u} \right) \quad (3)$$

The simplified motion equation for an incompressible Newtonian fluid with uniform viscosity:

$$\rho \frac{D\vec{u}}{Dt} = -\nabla p + \mu \nabla^2 \vec{u} + \rho \vec{g} \quad (4)$$

**Cartesian Coordinates** For a general fluid in cartesian coordinates:

$$\text{mass : } \frac{\partial \rho}{\partial t} + \frac{\partial(\rho u_x)}{\partial x} + \frac{\partial(\rho u_y)}{\partial y} + \frac{\partial(\rho u_z)}{\partial z} = 0 \quad (5)$$

$$\begin{aligned} \text{x-momentum : } \quad & \rho \left( \frac{\partial u_x}{\partial t} + u_x \frac{\partial u_x}{\partial x} + u_y \frac{\partial u_x}{\partial y} + u_z \frac{\partial u_x}{\partial z} \right) = \\ & - \frac{\partial p}{\partial x} - \frac{\partial \tau_{xx}}{\partial x} - \frac{\partial \tau_{yx}}{\partial y} - \frac{\partial \tau_{zx}}{\partial z} + F_x \end{aligned} \quad (6)$$

$$\begin{aligned} \text{y-momentum : } \quad & \rho \left( \frac{\partial u_y}{\partial t} + u_x \frac{\partial u_y}{\partial x} + u_y \frac{\partial u_y}{\partial y} + u_z \frac{\partial u_y}{\partial z} \right) = \\ & - \frac{\partial p}{\partial y} - \frac{\partial \tau_{xy}}{\partial x} - \frac{\partial \tau_{yy}}{\partial y} - \frac{\partial \tau_{zy}}{\partial z} + F_y \end{aligned} \quad (7)$$

$$\begin{aligned} \text{z-momentum : } \quad & \rho \left( \frac{\partial u_z}{\partial t} + u_x \frac{\partial u_z}{\partial x} + u_y \frac{\partial u_z}{\partial y} + u_z \frac{\partial u_z}{\partial z} \right) = \\ & - \frac{\partial p}{\partial z} - \frac{\partial \tau_{xz}}{\partial x} - \frac{\partial \tau_{yz}}{\partial y} - \frac{\partial \tau_{zz}}{\partial z} + F_z \end{aligned} \quad (8)$$

Shear stress constitutive equation:

$$\tau_{xx} = -\mu \left( 2 \frac{\partial u_x}{\partial x} - \frac{2}{3} \nabla \cdot \vec{u} \right) \quad (9)$$

$$\tau_{yy} = -\mu \left( 2 \frac{\partial u_y}{\partial y} - \frac{2}{3} \nabla \cdot \vec{u} \right) \quad (10)$$

$$\tau_{zz} = -\mu \left( 2 \frac{\partial u_z}{\partial z} - \frac{2}{3} \nabla \cdot \vec{u} \right) \quad (11)$$

$$\tau_{xy} = \tau_{yx} = -\mu \left( \frac{\partial u_x}{\partial y} + \frac{\partial u_y}{\partial x} \right) \quad (12)$$

$$\tau_{xz} = \tau_{zx} = -\mu \left( \frac{\partial u_x}{\partial z} + \frac{\partial u_z}{\partial x} \right) \quad (13)$$

$$\tau_{yz} = \tau_{zy} = -\mu \left( \frac{\partial u_y}{\partial z} + \frac{\partial u_z}{\partial y} \right) \quad (14)$$

$$\nabla \cdot \vec{u} = \frac{\partial u_x}{\partial x} + \frac{\partial u_y}{\partial y} + \frac{\partial u_z}{\partial z} \quad (15)$$

For a Newtonian incompressible fluid in cartesian coordinates:

$$\begin{aligned} \text{x-momentum : } \quad & \rho \left( \frac{\partial u_x}{\partial t} + u_x \frac{\partial u_x}{\partial x} + u_y \frac{\partial u_x}{\partial y} + u_z \frac{\partial u_x}{\partial z} \right) = \\ & - \frac{\partial p}{\partial x} + \mu \left( \frac{\partial^2 u_x}{\partial x^2} + \frac{\partial^2 u_x}{\partial y^2} + \frac{\partial^2 u_x}{\partial z^2} \right) + F_x \end{aligned} \quad (16)$$

$$\begin{aligned} \text{y-momentum : } \quad & \rho \left( \frac{\partial u_y}{\partial t} + u_x \frac{\partial u_y}{\partial x} + u_y \frac{\partial u_y}{\partial y} + u_z \frac{\partial u_y}{\partial z} \right) = \\ & - \frac{\partial p}{\partial y} + \mu \left( \frac{\partial^2 u_y}{\partial x^2} + \frac{\partial^2 u_y}{\partial y^2} + \frac{\partial^2 u_y}{\partial z^2} \right) + F_y \end{aligned} \quad (17)$$

$$\begin{aligned} \text{z-momentum : } \quad & \rho \left( \frac{\partial u_z}{\partial t} + u_x \frac{\partial u_z}{\partial x} + u_y \frac{\partial u_z}{\partial y} + u_z \frac{\partial u_z}{\partial z} \right) = \\ & - \frac{\partial p}{\partial z} + \mu \left( \frac{\partial^2 u_z}{\partial x^2} + \frac{\partial^2 u_z}{\partial y^2} + \frac{\partial^2 u_z}{\partial z^2} \right) + F_z \end{aligned} \quad (18)$$

**Cylindrical Coordinates** For a general fluid in cylindrical coordinates:

$$\text{mass : } \frac{\partial \rho}{\partial t} + \frac{1}{r} \frac{\partial}{\partial r} (\rho r u_r) + \frac{1}{r} \frac{\partial}{\partial \theta} (\rho u_\theta) + \frac{\partial}{\partial z} (\rho u_z) = 0 \quad (19)$$

$$\begin{aligned} r\text{-momentum : } \rho \left( \frac{\partial u_r}{\partial t} + u_r \frac{\partial u_r}{\partial r} + \frac{u_\theta}{r} \frac{\partial u_r}{\partial \theta} - \frac{u_\theta^2}{r} + u_z \frac{\partial u_r}{\partial z} \right) = \\ - \frac{\partial p}{\partial r} - \left( \frac{1}{r} \frac{\partial}{\partial r} (r \tau_{rr}) + \frac{1}{r} \frac{\partial \tau_{r\theta}}{\partial \theta} - \frac{\tau_{\theta\theta}}{r} + \frac{\partial \tau_{rz}}{\partial z} \right) + F_r \end{aligned} \quad (20)$$

$$\begin{aligned} \theta\text{-momentum : } \rho \left( \frac{\partial u_\theta}{\partial t} + u_r \frac{\partial u_\theta}{\partial r} + \frac{u_\theta}{r} \frac{\partial u_\theta}{\partial \theta} + \frac{u_r u_\theta}{r} + u_z \frac{\partial u_\theta}{\partial z} \right) = \\ - \frac{1}{r} \frac{\partial p}{\partial \theta} - \left( \frac{1}{r^2} \frac{\partial}{\partial r} (r^2 \tau_{r\theta}) + \frac{1}{r} \frac{\partial \tau_{\theta\theta}}{\partial \theta} + \frac{\partial \tau_{\theta z}}{\partial z} \right) + F_\theta \end{aligned} \quad (21)$$

$$\begin{aligned} z\text{-momentum : } \rho \left( \frac{\partial u_z}{\partial t} + u_r \frac{\partial u_z}{\partial r} + \frac{u_\theta}{r} \frac{\partial u_z}{\partial \theta} + u_z \frac{\partial u_z}{\partial z} \right) = \\ - \frac{\partial p}{\partial z} - \left( \frac{1}{r} \frac{\partial}{\partial r} (r \tau_{rz}) + \frac{1}{r} \frac{\partial \tau_{\theta z}}{\partial \theta} + \frac{\partial \tau_{zz}}{\partial z} \right) + F_z \end{aligned} \quad (22)$$

Shear stress constitutive equation:

$$\tau_{rr} = -\mu \left( 2 \frac{\partial u_r}{\partial r} - \frac{2}{3} (\nabla \cdot \vec{u}) \right) \quad (23)$$

$$\tau_{\theta\theta} = -\mu \left( 2 \left( \frac{1}{r} \frac{\partial u_\theta}{\partial \theta} + \frac{u_r}{r} \right) - \frac{2}{3} (\nabla \cdot \vec{u}) \right) \quad (24)$$

$$\tau_{zz} = -\mu \left( 2 \frac{\partial u_z}{\partial z} - \frac{2}{3} (\nabla \cdot \vec{u}) \right) \quad (25)$$

$$\tau_{r\theta} = \tau_{\theta r} = -\mu \left( r \frac{\partial}{\partial r} \left( \frac{u_\theta}{r} \right) + \frac{1}{r} \frac{\partial u_r}{\partial \theta} \right) \quad (26)$$

$$\tau_{rz} = \tau_{zr} = -\mu \left( \frac{\partial u_z}{\partial r} + \frac{\partial u_r}{\partial z} \right) \quad (27)$$

$$\tau_{\theta z} = \tau_{z\theta} = -\mu \left( \frac{\partial u_\theta}{\partial z} + \frac{1}{r} \frac{\partial u_z}{\partial \theta} \right) \quad (28)$$

$$\nabla \cdot \vec{u} = \frac{1}{r} \frac{\partial}{\partial r} (r u_r) + \frac{1}{r} \frac{\partial u_\theta}{\partial \theta} + \frac{\partial u_z}{\partial z} \quad (29)$$

For a Newtonian incompressible fluid in cylindrical coordinates:

$$r\text{-momentum : } \rho \left( \frac{\partial u_r}{\partial t} + u_r \frac{\partial u_r}{\partial r} + \frac{u_\theta}{r} \frac{\partial u_r}{\partial \theta} - \frac{u_\theta^2}{r} + u_z \frac{\partial u_r}{\partial z} \right) = \quad (30)$$

$$- \frac{\partial p}{\partial r} + \mu \left[ \frac{\partial}{\partial r} \left( \frac{1}{r} \frac{\partial}{\partial r} (r u_r) \right) + \frac{1}{r^2} \frac{\partial^2 u_r}{\partial \theta^2} - \frac{2}{r^2} \frac{\partial u_\theta}{\partial \theta} + \frac{\partial^2 u_r}{\partial z^2} \right] + F_r$$

$$\theta\text{-momentum : } \rho \left( \frac{\partial u_\theta}{\partial t} + u_r \frac{\partial u_\theta}{\partial r} + \frac{u_\theta}{r} \frac{\partial u_\theta}{\partial \theta} + \frac{u_r u_\theta}{r} + u_z \frac{\partial u_\theta}{\partial z} \right) = \quad (31)$$

$$- \frac{1}{r} \frac{\partial p}{\partial \theta} + \mu \left[ \frac{\partial}{\partial r} \left( \frac{1}{r} \frac{\partial}{\partial r} (r u_\theta) \right) + \frac{1}{r^2} \frac{\partial^2 u_\theta}{\partial \theta^2} + \frac{2}{r^2} \frac{\partial u_r}{\partial \theta} + \frac{\partial^2 u_\theta}{\partial z^2} \right] + F_\theta$$

$$z\text{-momentum : } \rho \left( \frac{\partial u_z}{\partial t} + u_r \frac{\partial u_z}{\partial r} + \frac{u_\theta}{r} \frac{\partial u_z}{\partial \theta} + u_z \frac{\partial u_z}{\partial z} \right) = \quad (32)$$

$$- \frac{\partial p}{\partial z} + \mu \left[ \frac{1}{r} \frac{\partial}{\partial r} \left( r \frac{\partial u_z}{\partial r} \right) + \frac{1}{r^2} \frac{\partial^2 u_z}{\partial \theta^2} + \frac{\partial^2 u_z}{\partial z^2} \right] + F_z$$

**Spherical Coordinates** For a general fluid in spherical coordinates:

$$\text{mass : } \frac{\partial \rho}{\partial t} + \frac{1}{r^2} \frac{\partial}{\partial r} (\rho r^2 u_r) + \frac{1}{r \sin \theta} \frac{\partial}{\partial \theta} (\rho u_\theta \sin \theta) + \frac{1}{r \sin \theta} \frac{\partial}{\partial \phi} (\rho u_\phi) = 0 \quad (33)$$

$$\begin{aligned} \text{r-momentum : } \rho \left( \frac{\partial u_r}{\partial t} + u_r \frac{\partial u_r}{\partial r} + \frac{u_\theta}{r} \frac{\partial u_r}{\partial \theta} + \frac{u_\phi}{r \sin \theta} \frac{\partial u_r}{\partial \phi} - \frac{u_\theta^2 + u_\phi^2}{r} \right) &= -\frac{\partial p}{\partial r} \\ &- \left( \frac{1}{r^2} \frac{\partial}{\partial r} (r^2 \tau_{rr}) + \frac{1}{r \sin \theta} \frac{\partial}{\partial \theta} (\tau_{r\theta} \sin \theta) + \frac{1}{r \sin \theta} \frac{\partial \tau_{r\phi}}{\partial \phi} - \frac{\tau_{\theta\theta} + \tau_{\phi\phi}}{r} \right) + F_r \end{aligned} \quad (34)$$

$$\begin{aligned} \theta\text{-momentum : } \rho \left( \frac{\partial u_\theta}{\partial t} + u_r \frac{\partial u_\theta}{\partial r} + \frac{u_\theta}{r} \frac{\partial u_\theta}{\partial \theta} + \frac{u_\phi}{r \sin \theta} \frac{\partial u_\theta}{\partial \phi} + \frac{u_\theta u_\phi}{r} - \frac{u_\phi \cot \theta}{r} \right) &= -\frac{1}{r} \frac{\partial p}{\partial \theta} \\ &- \left( \frac{1}{r^2} \frac{\partial}{\partial r} (r^2 \tau_{r\theta}) + \frac{1}{r \sin \theta} \frac{\partial}{\partial \theta} (\tau_{\theta\theta} \sin \theta) + \frac{1}{r \sin \theta} \frac{\partial \tau_{\theta\phi}}{\partial \phi} + \frac{\tau_{r\theta}}{r} - \frac{\tau_{\phi\phi} \cot \theta}{r} \right) + F_\theta \end{aligned} \quad (35)$$

$$\begin{aligned} \phi\text{-momentum : } \rho \left( \frac{\partial u_\phi}{\partial t} + u_r \frac{\partial u_\phi}{\partial r} + \frac{u_\theta}{r} \frac{\partial u_\phi}{\partial \theta} + \frac{u_\phi}{r \sin \theta} \frac{\partial u_\phi}{\partial \phi} + \frac{u_\phi u_r}{r} + \frac{u_\theta u_\phi \cot \theta}{r} \right) &= -\frac{1}{r \sin \theta} \frac{\partial p}{\partial \phi} \\ &- \left( \frac{1}{r^2} \frac{\partial}{\partial r} (r^2 \tau_{r\phi}) + \frac{1}{r} \frac{\partial \tau_{\theta\phi}}{\partial \theta} + \frac{1}{r \sin \theta} \frac{\partial \tau_{\phi\phi}}{\partial \phi} + \frac{\tau_{r\phi}}{r} + \frac{2\tau_{\theta\phi} \cot \theta}{r} \right) + F_\phi \end{aligned} \quad (36)$$

Shear stress constitutive equation:

$$\tau_{rr} = -\mu \left( 2 \frac{\partial u_r}{\partial r} - \frac{2}{3} (\nabla \cdot \vec{u}) \right) \quad (37)$$

$$\tau_{\theta\theta} = -\mu \left( 2 \left( \frac{1}{r} \frac{\partial u_\theta}{\partial \theta} + \frac{u_r}{r} \right) - \frac{2}{3} (\nabla \cdot \vec{u}) \right) \quad (38)$$

$$\tau_{\phi\phi} = -\mu \left( 2 \left( \frac{1}{r \sin \theta} \frac{\partial u_\phi}{\partial \phi} + \frac{u_r}{r} + \frac{u_\theta \cot \theta}{r} \right) - \frac{2}{3} (\nabla \cdot \vec{u}) \right) \quad (39)$$

$$\tau_{r\theta} = \tau_{\theta r} = -\mu \left( r \frac{\partial}{\partial r} \left( \frac{u_\theta}{r} \right) + \frac{1}{r} \frac{\partial u_r}{\partial \theta} \right) \quad (40)$$

$$\tau_{r\phi} = \tau_{\phi r} = -\mu \left( \frac{1}{r \sin \theta} \frac{\partial u_r}{\partial \phi} + r \frac{\partial}{\partial r} \left( \frac{u_\phi}{r} \right) \right) \quad (41)$$

$$\tau_{\theta\phi} = \tau_{\phi\theta} = -\mu \left( \frac{\sin \theta}{r} \frac{\partial}{\partial \theta} \left( \frac{u_\phi}{\sin \theta} \right) + \frac{1}{r \sin \theta} \frac{\partial u_\theta}{\partial \phi} \right) \quad (42)$$

$$\nabla \cdot \vec{u} = \frac{1}{r^2} \frac{\partial}{\partial r} (r^2 u_r) + \frac{1}{r \sin \theta} \frac{\partial}{\partial \theta} (u_\theta \sin \theta) + \frac{1}{r \sin \theta} \frac{\partial u_\phi}{\partial \phi} \quad (43)$$



For a Newtonian incompressible fluid in spherical coordinates:

$$r\text{-momentum: } \rho \left( \frac{\partial u_r}{\partial t} + u_r \frac{\partial u_r}{\partial r} + \frac{u_\theta}{r} \frac{\partial u_r}{\partial \theta} + \frac{u_\phi}{r \sin \theta} \frac{\partial u_r}{\partial \phi} - \frac{u_\theta^2 + u_\phi^2}{r} \right) = -\frac{\partial p}{\partial r} \quad (44)$$

$$+ \mu \left( \frac{1}{r^2} \frac{\partial^2}{\partial r^2} (r^2 u_r) + \frac{1}{r^2 \sin \theta} \frac{\partial}{\partial \theta} \left( \sin \theta \frac{\partial u_r}{\partial \theta} \right) + \frac{1}{r^2 \sin^2 \theta} \frac{\partial^2 u_r}{\partial \phi^2} \right) + F_r$$

$$\theta\text{-momentum: } \rho \left( \frac{\partial u_\theta}{\partial t} + u_r \frac{\partial u_\theta}{\partial r} + \frac{u_\theta}{r} \frac{\partial u_\theta}{\partial \theta} + \frac{u_\phi}{r \sin \theta} \frac{\partial u_\theta}{\partial \phi} + \frac{u_\theta u_\phi}{r} - \frac{u_\phi \cot \theta}{r} \right) = -\frac{1}{r} \frac{\partial p}{\partial \theta} \quad (45)$$

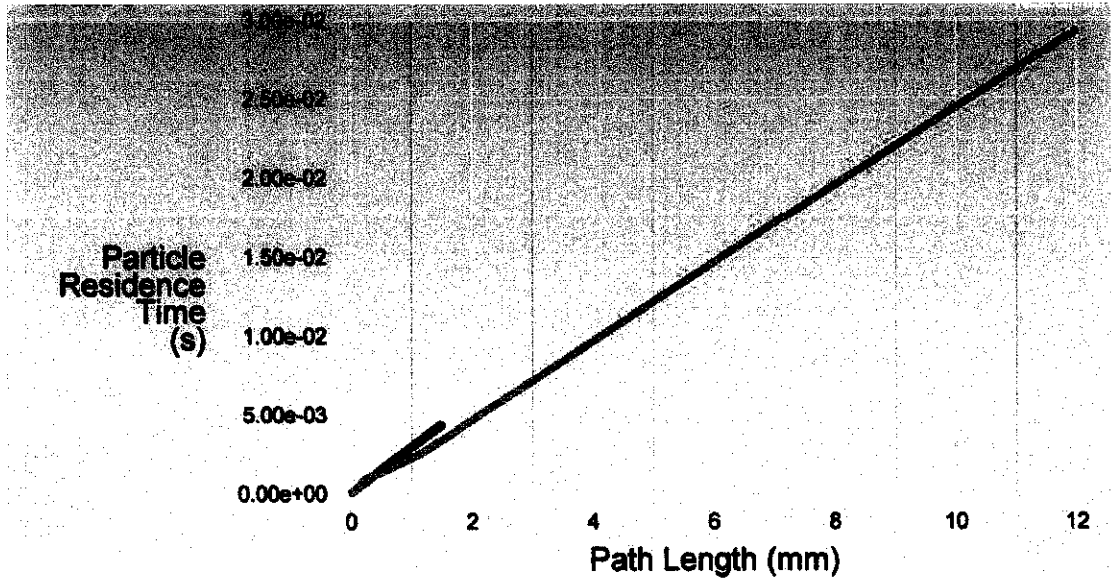
$$+ \mu \left( \frac{1}{r^2} \frac{\partial}{\partial r} \left( r^2 \frac{\partial u_\theta}{\partial r} \right) + \frac{1}{r^2} \frac{\partial}{\partial \theta} \left( \frac{1}{\sin \theta} \frac{\partial}{\partial \theta} (u_\theta \sin \theta) \right) + \frac{1}{r^2 \sin^2 \theta} \frac{\partial^2 u_\theta}{\partial \phi^2} \right. \\ \left. + \frac{2}{r^2} \frac{\partial u_r}{\partial \theta} - \frac{2 \cos \theta}{r^2 \sin^2 \theta} \frac{\partial u_\phi}{\partial \phi} \right) + F_\theta$$

$$\phi\text{-momentum: } \rho \left( \frac{\partial u_\phi}{\partial t} + u_r \frac{\partial u_\phi}{\partial r} + \frac{u_\theta}{r} \frac{\partial u_\phi}{\partial \theta} + \frac{u_\phi}{r \sin \theta} \frac{\partial u_\phi}{\partial \phi} + \frac{u_\phi u_r}{r} + \frac{u_\theta u_\phi \cot \theta}{r} \right) = -\frac{1}{r \sin \theta} \frac{\partial p}{\partial \phi} \quad (46)$$

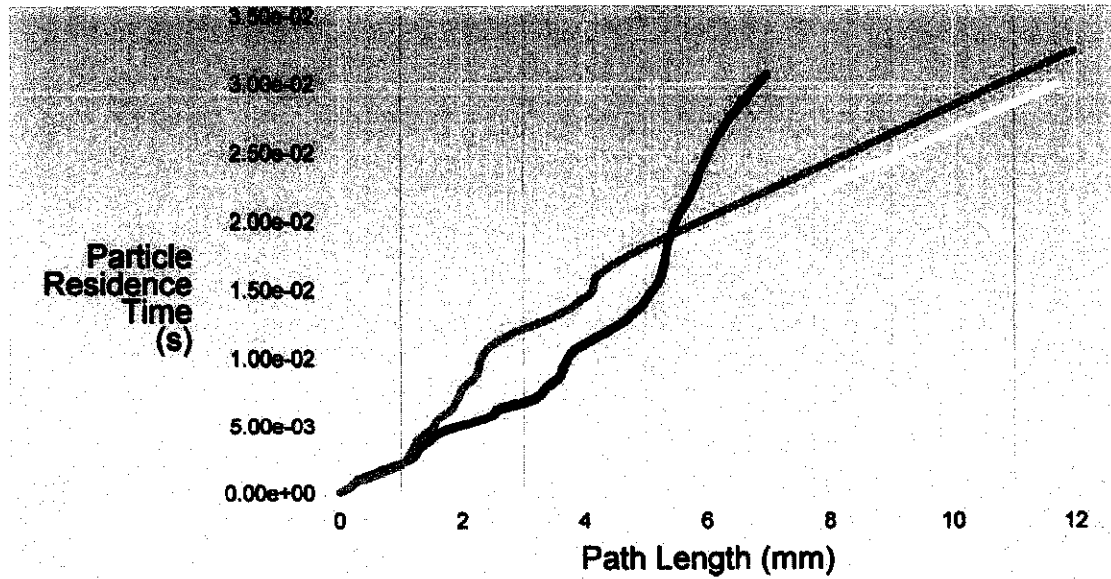
$$+ \mu \left( \frac{1}{r^2} \frac{\partial}{\partial r} \left( r^2 \frac{\partial u_\phi}{\partial r} \right) + \frac{1}{r^2} \frac{\partial}{\partial \theta} \left( \frac{1}{\sin \theta} \frac{\partial}{\partial \theta} (u_\phi \sin \theta) \right) + \frac{1}{r^2 \sin^2 \theta} \frac{\partial^2 u_\phi}{\partial \phi^2} \right. \\ \left. + \frac{2}{r^2 \sin \theta} \frac{\partial u_r}{\partial \phi} - \frac{2 \cos \theta}{r^2 \sin^2 \theta} \frac{\partial u_\theta}{\partial \phi} \right) + F_\phi$$

### C1) XY PLOT OF PATH LENGTH (MM) VERSUS PARTICLE RESIDENCE TIME


- Path Length (mm) Versus Particle Residence Time at Inlet 0.4 m/s



- Path Length (mm) Versus Particle Residence Time at Inlet 0.5 m/s



**D1) VIVA Slide Presentation**




UNIVERSITI  
PETRONAS

# Accumulation of Low Density Lipoprotein (LDL) in Diseased Artery

By:  
**Nurulain Amelia binti Mohd Razmi**  
11194  
Supervisor: **Dr Anis Suhaila bt Shuib**

Chemical Engineering  
Generating Futures



UNIVERSITI  
PETRONAS

## Presentation Outline

- INTRODUCTION
- PROBLEM STATEMENT
- OBJECTIVES & SCOPE OF STUDY
- LITERATURE REVIEW & THEORY
- METHODOLOGY
- RESULT & DISCUSSION
- CONCLUSION & RECOMENDATION

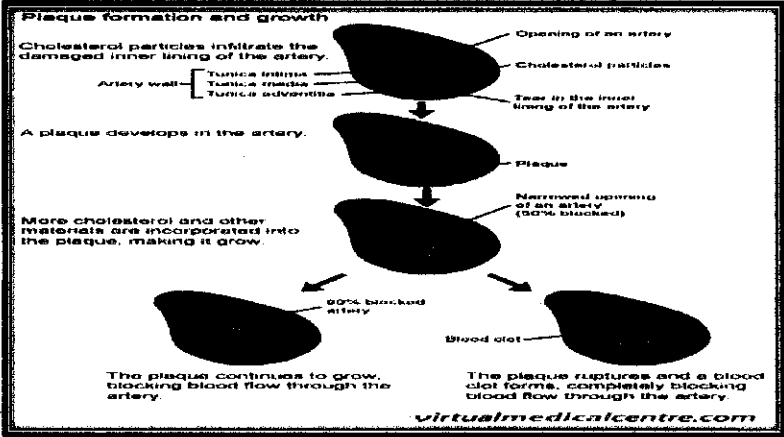
Chemical Engineering  
Generating Futures

# Atherosclerosis



Lead to the formation of plaque

Narrow the artery

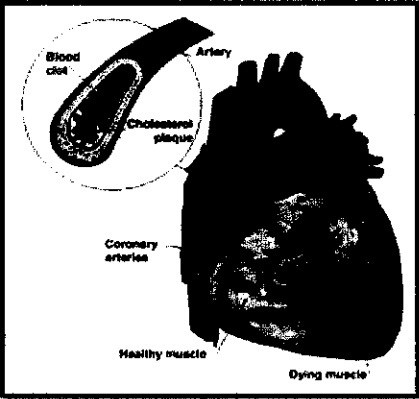
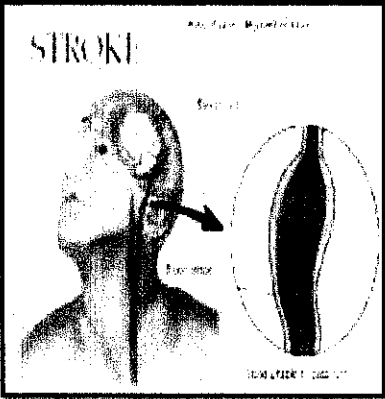


3



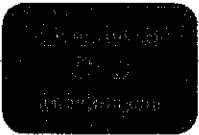
**CVD**

Cardiovascular disease (CVD) is group of disorder of heart and blood vessel and become the number one cause of death globally.



4





• In 2009, one in four death in government hospital suffered from heart and stroke.

10 Sebab Kematian utama, Malaysia, 2006 10 Principal Causes of Death, Malaysia, 2006			
Disahkan Medically certified	%	Tidak disahkan Not medically certified	%
1. Ischaemic heart disease	12.0	1. Sakit tua 65+ Old age 65+	57.9
2. Septicaemia	7.1	2. Lelah Asthma	7.3
3. Cerebrovascular disease	7.0	3. Barah Cancer	7.1
4. Transport accident	5.7	4. Sakit jantung Heart disease	5.8
5. Pneumonia	5.4	5. Kencing manis Diabetes	3.5
6. Chronic lower respiratory disease	2.4	6. Jangkitan kuman Viral Infection	2.4
7. Malignant neoplasm of trachea, bronchus and lung	2.2	7. Darah tinggi Hypertension	1.7
8. Diabetes mellitus	2.1	8. Angin xhwar Stroke	1.2
9. Certain conditions originating in the perinatal period	1.8	9. Penyakit berjangkit Infectious disease	1.0
10. Congenital malformations, deformations and chromosomal abnormalities	1.4	10. Sakit buah pinggang Kidney disease	1.0
Keseluruhan sebab All causes (68,124)		Keseluruhan sebab All causes (46,960)	

Department of Statistics Malaysia.

Dr Choo Gim Hooi. (2012). Predicting heart disease risks. Retrieved February 8, 2012, from <http://thestar.com.my/health/story.asp?file=/2012/2/5/health/10665267&sec=health>

## Problem Statement



The blood flow is a pulsatile in nature. The interest of knowing to what extent of velocity varies in LDL accumulation.

Another factor that may effect the atherosclerosis is LDL size and it still remain debatable.

## DISCIPLINE STUDY

<p>The effect of LDL accumulation is inspected with these objectives :</p> <ul style="list-style-type: none"> <li>• To study the effect of velocity changes in LDL accumulation.</li> <li>• To investigate the effect of LDL sizes that corresponding to LDL accumulation.</li> </ul>	<ul style="list-style-type: none"> <li>• Simulated using ANSYS 14.0</li> <li>• Involved an artery model with 30% reduction to represent a diseased artery.</li> </ul>
---	---

## Blood flow behavior

- Blood flow in artery is corresponded to a shear stress
- Can be described by the theory of viscosity.

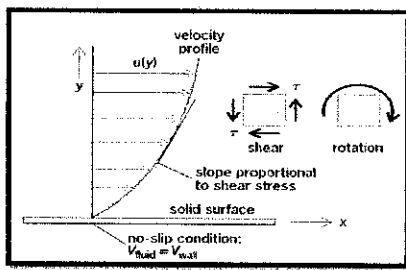


Figure 1: the velocity gradient

### Newton's Law of Viscosity

$$\tau_w = \mu \cdot \dot{\gamma}_w \quad (1)$$

$\tau$  = shear stress

$\mu$  = viscosity

$\dot{\gamma}_w$  = shear rate (velocity gradient)

White, F.M. (2008). *Fluid mechanics*. Retrieved February 20, 2012, from <http://accessscience.com/content/Fluid-mechanics/262300>  
 Katrasis, D., et al. (2007). Wall shear stress: Theoretical considerations and methods of measurement. *Progress in Cardiovascular Diseases*, 49(5), 307-329.

## Hagen Poiseuille Law



- Expresses the relationship between the rate of flow of a liquid in a tube and the pressure gradient in the tube, the radius of the tube, the length of the tube and the viscosity of the liquid.

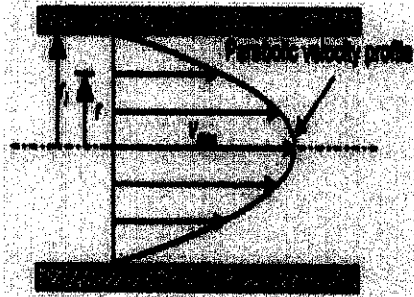


Figure 2: Hagen Poiseuille Flow Concept

In a case of laminar and steady flow.

$$v_r = \frac{\Delta P (r_i^2 - r^2)}{4 \eta l}$$



Blood flowrate

$$Q = \frac{\Delta P \pi r_i^4}{8 \eta l}$$

## Navier Stoke Equation



- Navier stokes Equation is equation to describe the flow of fluid in whatever geometry either straight tube, cylindrical tube and et cetera

$$\rho \frac{DV}{Dt} = -\nabla P + \mu \nabla^2 V + \rho g \quad (2)$$

Local acceleration      Pressure force per unit volume      Viscous forces per unit volume      Body force per unit volume



## Particle Motion Equation



- Lipid is a spherical particle and can be described as equation below:

$$m_p \frac{dv_p}{dt} = m_p \left( 1 - \frac{\rho}{\rho_p} \right) g + F_{PG} + F_D + F_L + F_{VM} + F_{Bas}$$

particle inertia

forces caused by particle fluid interaction.

16

## Modeling blood flow



- Easy to be constructed
- Can be reproduced
- The boundary condition can be varied
- More convenient and comprehensive result

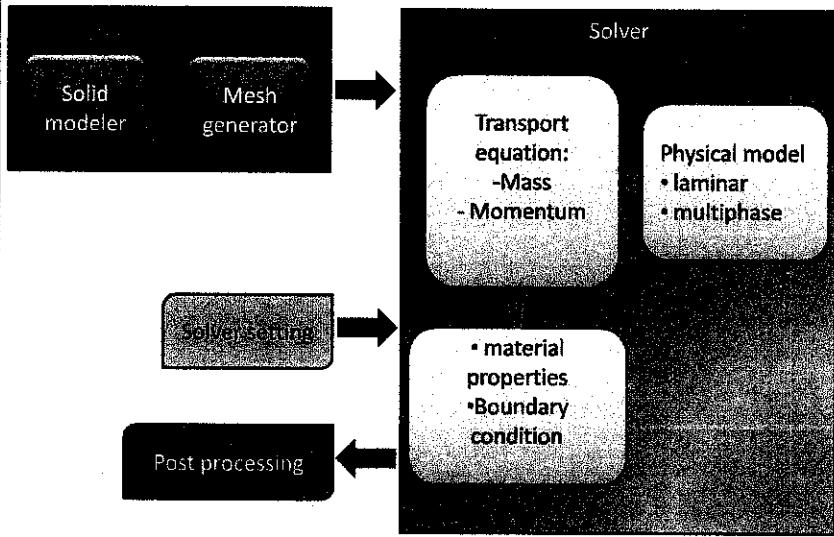
Reference: Shuib A, et.al (2010), Flow Regime Characterization in a Diseased Artery Model, *World Academy of Science, Engineering and Technology*, 62

17

# FLUENT Operation System



Chemical Engineering  
Generating Fuels



19

Chemical Engineering  
Generating Fuels

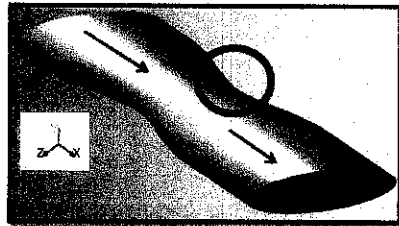


Figure 3: Diseased Artery Geometry

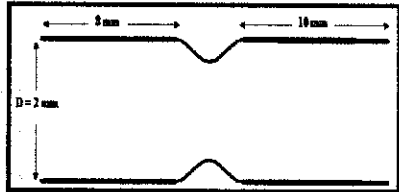


Figure 4: Normalised Scale

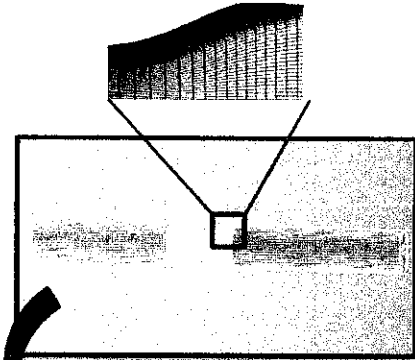


Figure 5: Meshing

Cells : 464437  
Nodes: 475661  
Faces: 1404111

20

Solver setting



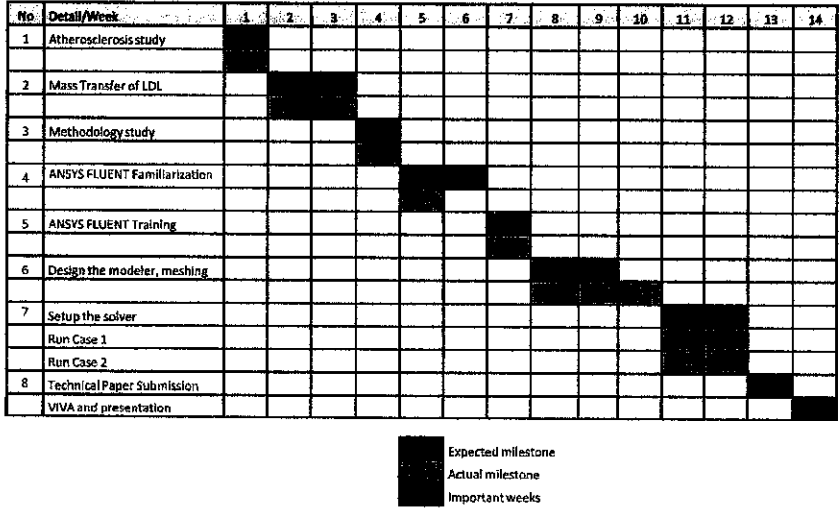
<b>Inlet velocity</b>	•0.18 m/s, 0.20 m/s, 0.3 m/s, 0.4 m/s, 0.5 m/s
<b>Physical models</b>	Viscous model •Spalart allmaras •Discrete phase
<b>Blood properties</b>	Density: 1060 kg/m <sup>3</sup> Viscosity: 0.004 kg/m.s
<b>LDL property</b>	Density: 1050 kg/m <sup>3</sup> LDL sizes: 1 μm, 3 μm, 5 μm [1]

Solution methods

Pressure velocity coupling	SIMPLEC
Pressure	Standard
Momentum	Second Order Upwind
Modified Turbulent Viscosity	2 <sup>nd</sup> Order Upwind

[1] Trippel G, et al (2011). CFD Modeling of an Ultrasonic Separator for the Removal of Lipid Particles From Pericardial Suction Blood. *IEEE Transactions on Biomedical Engineering*, Vol 58, No.2. 21

## Project Milestone FYP GANTT CHART



# Recirculation Region Study



Chemical Engineering  
Separating Units

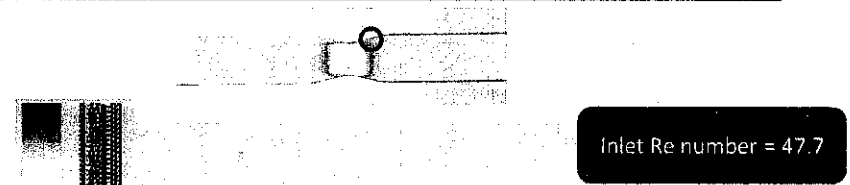


Figure 6: Velocity vector at inlet velocity 0.18 m/s

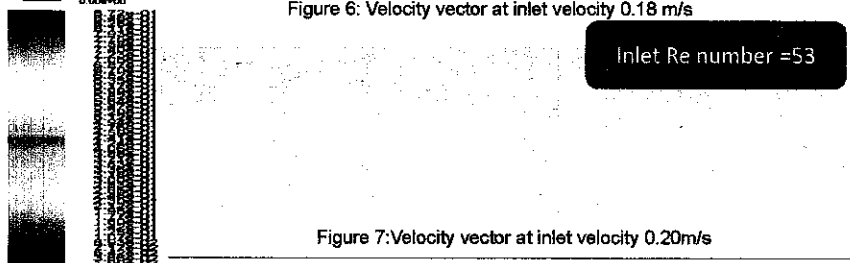


Figure 7: Velocity vector at inlet velocity 0.20 m/s

24

Chemical Engineering  
Separating Units



Figure 8: Velocity vector at inlet velocity 0.30 m/s

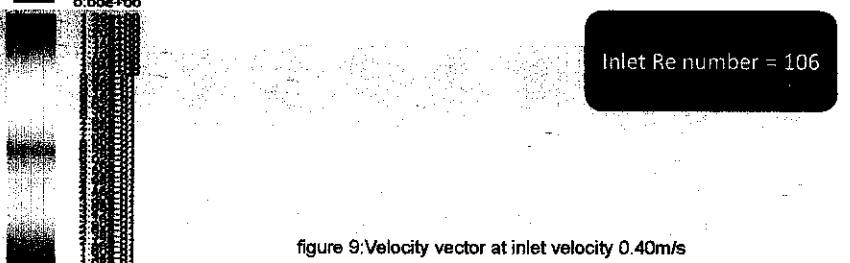


figure 9: Velocity vector at inlet velocity 0.40 m/s

25

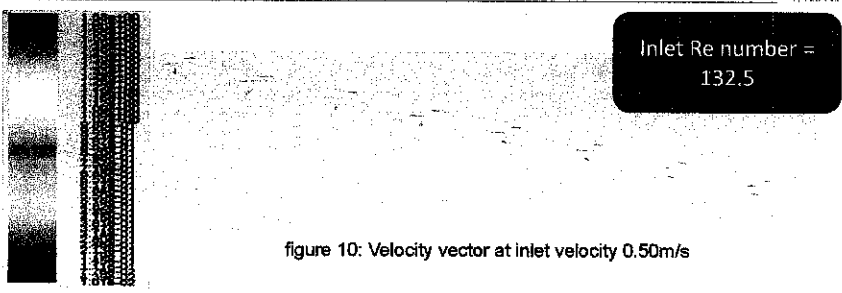


figure 10: Velocity vector at inlet velocity 0.50m/s

## LDL particle residence time study

The study of LDL particle residence time is simulated at three different positions

- 1)  $x = 0.4\text{mm}, y = 0, z = -0.71\text{mm}$
- 2)  $x = 0.4\text{mm}, y = 0, z = -0.70\text{mm}$
- 3)  $x = 0.4\text{mm}, y = 0, z = -0.65\text{mm}$

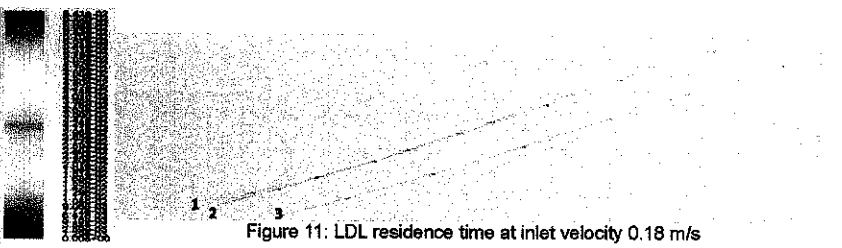


Figure 11: LDL residence time at inlet velocity 0.18 m/s

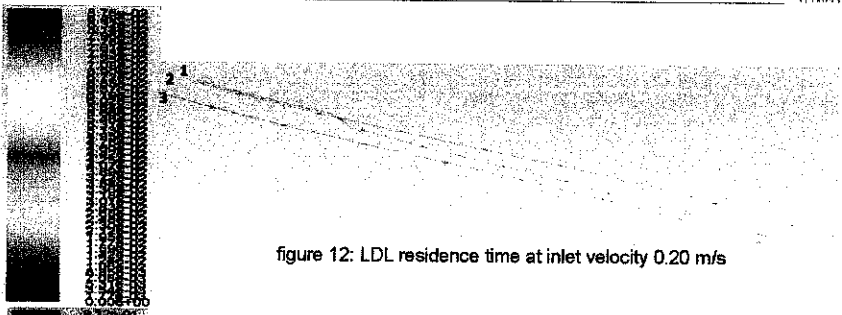


figure 12: LDL residence time at inlet velocity 0.20 m/s

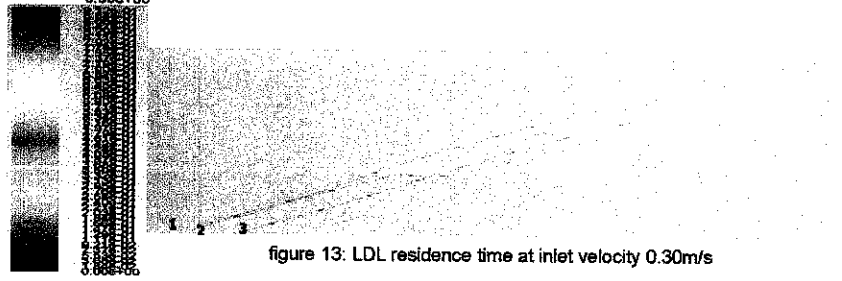


figure 13: LDL residence time at inlet velocity 0.30m/s

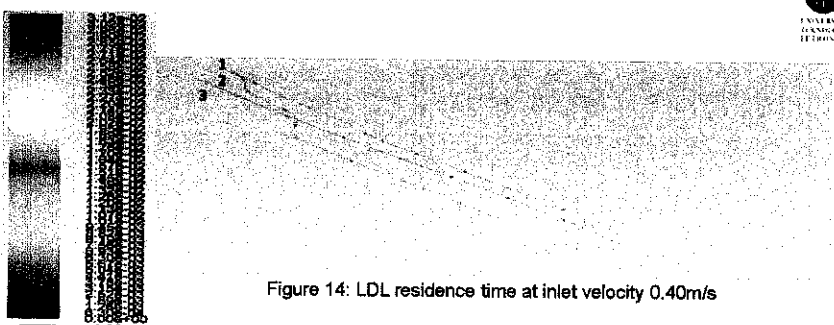


Figure 14: LDL residence time at inlet velocity 0.40m/s

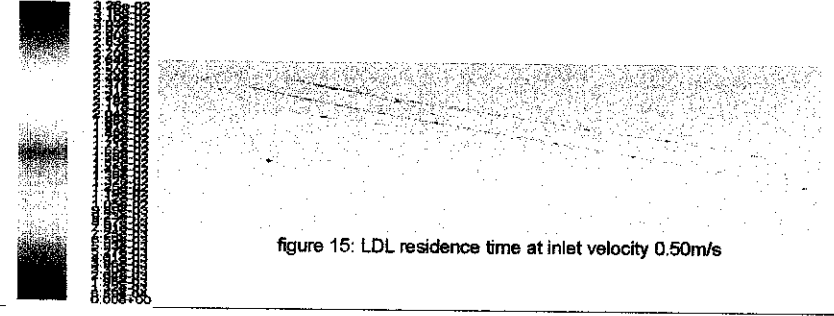


figure 15: LDL residence time at inlet velocity 0.50m/s

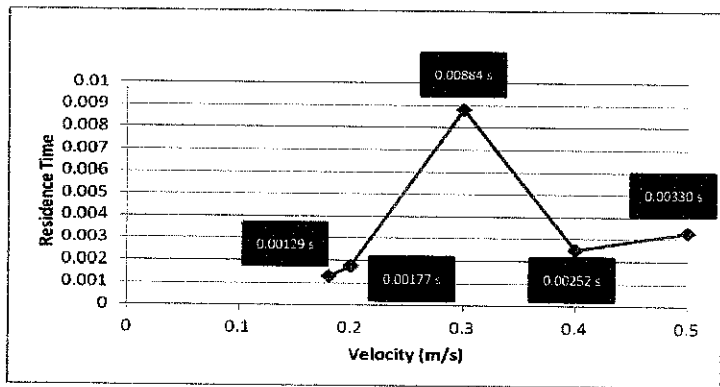


Figure 16: Graph of velocity versus residence time at recirculation region.

The LDL at these three velocities keeps longer at expected area as it create recirculation region.

### The Study of Lipid Size Variation in Corresponding To Lipid Accumulation.

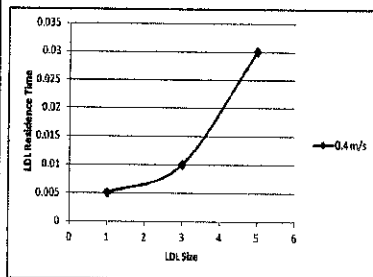


Figure 17 : Graph of LDL size versus LDL residence time at inlet velocity 0.4 m/s

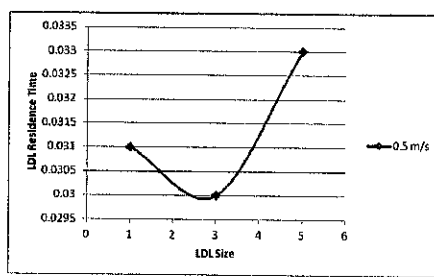


Figure 18 : Graph of LDL size versus LDL residence time at inlet velocity 0.5 m/s

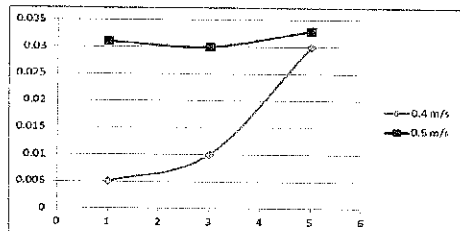


Figure 19: LDL size versus LDL residence time at two velocities

## Conclusion



The characteristic of blood flow can be determined from inlet Reynolds (Re) number. As the inlet velocity increased, the Re number increased as well. Thus, it describes the formation of recirculation region.

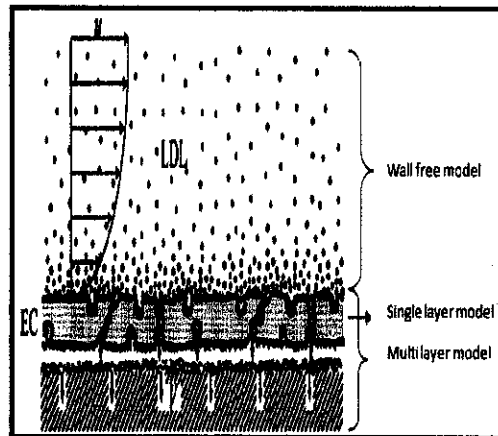
The large LDL size has the momentum that is bigger compare to small LDL size. therefore, it has low velocity and will stay longer at area of study.

The high velocity will create a recirculation region and has longer residence time of LDL at recirculation region. Thus, residence time has contributed to the formation of plaque by LDL.

## Recommendation



Taking into consideration about mass transfer of LDL into porous media.



Sun, N., Wood, N. B., Hughes, A. D., Thom, S. A. M., & Yun Xu, X. (2007b). Effects of transmural pressure and wall shear stress on LDL accumulation in the arterial wall: A numerical study using a multilayered model. *American Journal of Physiology-Heart and Circulatory Physiology*, 292(6), H3148-H3157.



## REFERENCES



- Bird, R. B. (2002). The equations of change for isothermal systems. In *Transport phenomena* (2nd edition ed., pp. 98-98). New York: John Wiley.
- *Cardiovascular diseases (CVDs)*. (2011). Retrieved February 10, 2012, from <http://www.who.int/mediacentre/factsheets/fs317/en/>
- Chakravarty, S., Mandal, P. K., & Andersson, H. I. (2009). Mass transfer to blood flowing through arterial stenosis. *Zeitschrift Für Angewandte Mathematik Und Physik (ZAMP)*, 60(2), 299-323.
- Chapter 2, Law of Poiseuille. Retrieved July 6, 2012 from <http://www.buchhandel.de/WebApi1/GetMmo.asp?MmoId=999524&mmoType=PDF&isbn=9780387233451>
- Ethier, C. R. (2002). Computational modeling of mass transfer and links to atherosclerosis. *Annals of Biomedical Engineering*, 30(4), 461-471.
- Fournier, R. L. (2011). *Basic transport phenomena in biomedical engineering* CRC Press.
- Hooi, C. G. (2012). **Predicting heart disease risks**. Retrieved February 8, 2012, from <http://thestar.com.my/health/story.asp?file=/2012/2/5/health/10665267&sec=health>
- Ikbal, M. A., Chakravarty, S., & Mandal, P. (2010). Numerical simulation of mass transfer to micropolar fluid flow past a stenosed artery. *International Journal for Numerical Methods in Fluids*,

36

- Ethier, C. R. (2002). Computational modeling of mass transfer and links to atherosclerosis. *Annals of Biomedical Engineering*, 30(4), 461-471.
- Fournier, R. L. (1998). *Basic transport phenomena in biomedical engineering* CRC Press.
- Kaazempur-Mofrad, M., Wada, S., Myers, J., & Ethier, C. (2005). Mass transport and fluid flow in stenotic arteries: Axisymmetric and asymmetric models. *International Journal of Heat and Mass Transfer*, 48(21), 4510-4517.
- Katritsis, D., Kaiktsis, L., Chaniotis, A., Pantos, J., Efstathopoulos, E. P., & Marmarelis, V. (2007). Wall shear stress: Theoretical considerations and methods of measurement. *Progress in Cardiovascular Diseases*, 49(5), 307-329.
- Shires, G. L. (2011). *SHERWOOD NUMBER*. Retrieved February 20, 2012, from <http://www.thermopedia.com/content/1122/>

37



- Kaazempur-Mofrad, M., Wada, S., Myers, J., & Ethier, C. (2005). Mass transport and fluid flow in stenotic arteries: Axisymmetric and asymmetric models. *International Journal of Heat and Mass Transfer*, 48(21), 4510-4517.
- Katritsis, D., Kaiktsis, L., Chaniotis, A., Pantos, J., Efstathopoulos, E. P., & Marmarelis, V. (2007). Wall shear stress: Theoretical considerations and methods of measurement. *Progress in Cardiovascular Diseases*, 49(5), 307-329.
- Keith U.I, Vincent W.B, Stocker R & Walling C (1993). Autoxidation of lipids and antioxidant by  $\alpha$ -tocopherol and ubiquinol in homogeneous solution and in aqueous dispersions of lipids: Unrecognized consequences of lipid particle size as exemplified by oxidation of human low density lipoprotein. *Proc. Natl. Acad. Sci. USA*, 90, 45-49.
- Lantz, J., & Karlsson, M. (2012). Large eddy simulation of LDL surface concentration in a subject specific human aorta. *Journal of Biomechanics*, 45(3), 537-542.
- 

38



- Rizzo M & Bernies K. (2006). Low-density lipoprotein size and cardiovascular risk assessment. Oxford University Press on behalf of the Association of Physics
- Sacks F.M. & Campos H (2003). Low Density Lipoprotein Size and Cardiovascular Disease: A Reappraisal. *The Journal of Clinical Endocrinology & Metabolism* 88(10):4525-4532
- Shuib A et al (2012), Flow Regime Characterization in a Diseased Artery Model. *International Journal of Biological and Life Sciences*, 8:4, 234-238
- Sun, N., Wood, N. B., Hughes, A. D., Thom, S. A. M., & Xu, X. Y. (2007a). Influence of pulsatile flow on LDL transport in the arterial wall. *Annals of Biomedical Engineering*, 35(10), 1782-1790.
- Sun, N., Wood, N. B., Hughes, A. D., Thom, S. A. M., & Yun Xu, X. (2007b). Effects of transmural pressure and wall shear stress on LDL accumulation in the arterial wall: A numerical study using a multilayered model. *American Journal of Physiology-Heart and Circulatory Physiology*, 292(6), H3148-H3157.
- Superko HR & Gadesam RR (2008). Is it LDL particle size or number that correlates with risk for cardiovascular disease? *Curr Atheroscler Rep* 10, 377-385.
- Varady K.A et. al (2010), Improvement in LDL particle size and distribution by short term alternate day modified fasting in obese adults. *British Journal of Nutrition*, 105,580-583

39